Control of Nano Carbon Structure by Using Solution Plasma Process

ソリューションプラズマプロセスを用いたナノカーボンの構造制御

Hoonseung LEE

2016

Department of Material Science and Engineering,

Graduate School of Engineering,

Nagoya University

Contents Page

Abstract

Carbon is very interesting element due to different forms according to bonding structure. Recently, lots of researchers have given an attention on interesting graphitic carbon forms such as fullerene, carbon nano tube and graphene. These different carbon forms are considered as one of nano materials of future technology for semiconductor and superconductor.

Graphene, that it is one of carbon allotropes, was suggested theoretically by P.R. Wallace in 1947. However, in 1930, Lev Landau and R.E. Peierls insisted that 2 dimensional crystalline could not exist with stable state because atoms of in it are thermally unstable. After that, N.D. Mermin made free-standing 2-D crystal structure but this structure could be temporarily exist, which experiment firmly supported theory of Landau-Peierls. By the way, in 2004, A.K. Geim succeeded to exfoliate graphene from graphite by using scotch tape method [1], and then, properties and bandgap of graphene was evaluated. From this research, research of graphene has promoted to new era of carbon renaissance.

For mass production synthesis of graphene, the method of plasma discharge in liquid media is the most expected candidate. Especially, solution plasma process (SPP) is very useful method due to using low input energy and temperature in the reaction field. Under the low input energy and temperature, precursors are activated with keeping the molecular structure through C-H activation and react with other molecules, without decomposition of precursors. Therefore, the properties of synthesized carbon materials depend on the original structure of the precursor. In other words, we can design the synthesized materials by the selection of the precursors.

Chapter 1 begins with an overview of nano carbon materials to make much more understanding in the overall research. Next, the fundamental and applications of solution plasma process was given in detail. The purpose of this study is to produce graphitic carbon

structure by using SPP. Therefore, in this study, we synthesized and progress carbon materials in the various liquid media. In chapter 2, our study focused on structure control of nanocarbon and interpretation of phenomenon in plasma reaction field. The energy per pulse delivered in plasma was similar for both nanocarbon structures such as carbon onions and graphene flakes. However, the power delivered in plasma was much higher in the case of carbon onion synthesis. The main process to produce the carbon onions is carbon vaporization due to Joule effect and carbon recombination assisted by plasma. In order to produce graphene flakes, the graphite electrode was exfoliated in plasma.

In order to improve reliability research against fluctuation of carbon properties, Chapter 3 researches to graphitic carbon structure synthesized from benzene solvent by using solution plasma process and controlled, especially through adjusting electrode gap distances. This effect plays the important role as the main factor for discharge process in organic solution. TEM and diffraction images of EG 1 showed ordered graphitic layers and clear ring pattern compared with EG 0.25. The only adjustment of electrode gap distance from 0.25 mm to 1 mm had brought about approximately 400 times improvement of conductive property from 19k Ω·cm to 47 Ω·cm. From the result of CHN elemental analysis, H/C ratio decreased with decrease of resistance from 0.31 to 0.18. The increase of sp2 carbon domains in size may cause to improvement of conductivity.

For further improvement of carbon properties by increase of sp2 domains, Chapter 4 presents the effect of introducing solute having more π conjugated sites than benzene and nanocarbon formation mechanism. Through SPP, enhanced carbon materials with high crystallinity and electric conductivity were synthesized by introducing solutes in benzene solvent such as naphthalene and anthracene, which have π conjugated molecular structures. Little amount of solute gave a significant effect on lowering H/C ratio of obtained carbon, which developed crystallinity of 2 dimensional graphitic structure. In addition, carbon quantity increased as well with high concentration of solutes. Electric resistance of obtained carbon by introducing

anthracene was measured around 16.6 Ωcm, which value was 7 times lower than that of about 104 Ωcm from pure benzene solvent.

Finally, chapter 5 summarized and clarified phenomenon in the plasma discharge in reaction filed, and the way of controlling carbon crystallinity and structures. In this study, we have successfully synthesized conductive carbon having graphitic layers by SPP. The results observed that (1) SPP is a promising method for mass production of carbon and versatile for controlling properties of carbon, (2) conductivity of carbon drastically increased by introducing small amount of precursor having π conjugated sites in benzene and (3) capacity and durability of Li-air battery could be improved without change of properties by heat treatment like aggregation of metal particles and evaporation of nitrogen.

Chapter 1

General introduction

Chapter 1 – General introduction

1.1 Versatile element, Carbon

In 1953, for the first time Miller synthesized amino acid from inorganic substances such as hydrogen, water vapor, metane and ammonia in flask discharge tube by using 60 thousand current. After that, Fox synthesized protein from amino acid, Oparin produced corserbate in laboratory, which is more similar to living things. These historical researches made a chance to reveal one aspect of origin of life.

Carbon is 6^{th} light element among confirmed 114 elements in the universe. This element is not that common, which has been made when supernovas explored long long time ago. The mass portion of carbon in Sun is just 0.29 % and carbon in Earth is 12^{th} common element. However, carbon shows us wide range of chemical diversities, surprisingly. Almost everything among over 70 million chemical materials known to mankind is related to carbon. Many kinds of confirmed protein and DNA are over 60 million.

Shell electrons of carbon is four, which means that this element in enable to make more various compound than any other one as mentioned before. Many people say that we could not live without oxygen. However, they do not know we could not live without carbon. What on earth can carbon manipulate our livings?

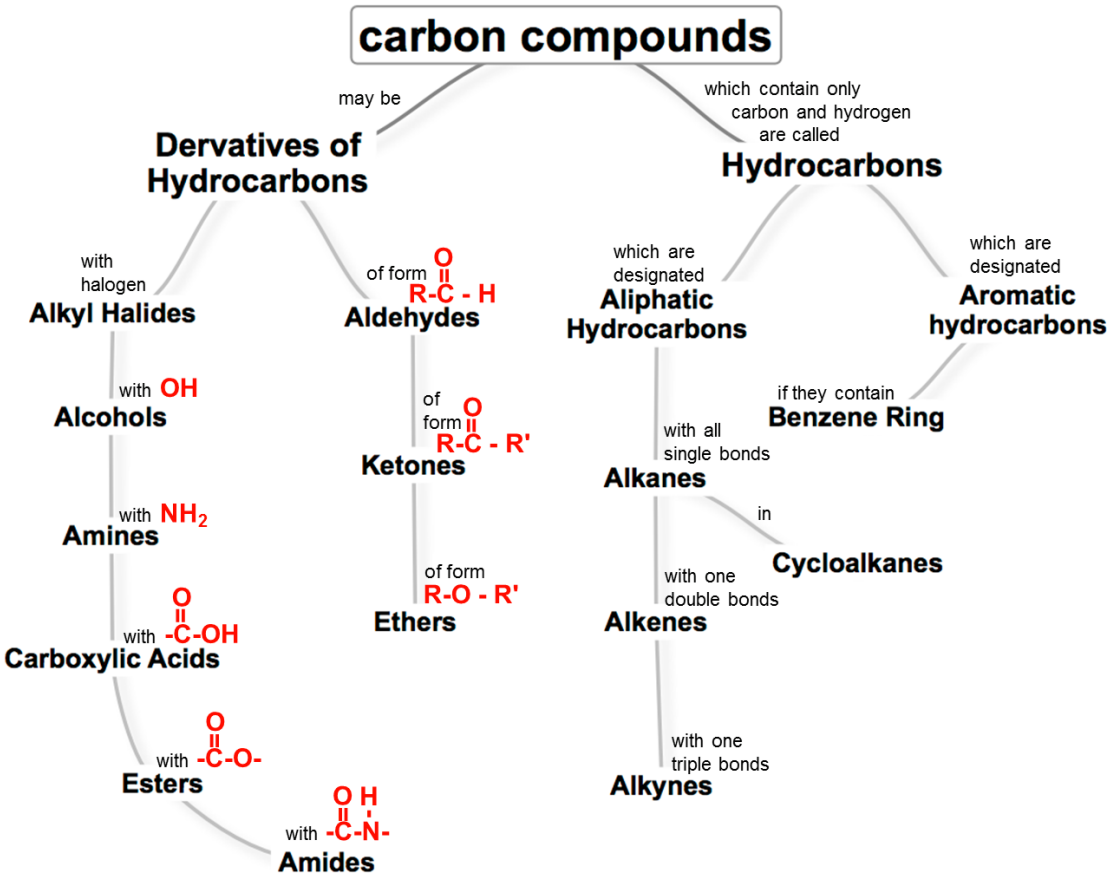

Fig. 1-1 Classification of carbon compounds

1.2 Definition of carbon compound

Carbon has 4 shell electrons. By arrangement of these electrons, carbon can show us its different appearance such as graphite or diamond. Graphite is a stacked structure with many layered sheets of hexagonal symmetry and sp^2 hybridization of the trigonally coordinated carbon atoms. On the contrary, diamond structure is tetrahedrally composed with sp3 hybridization of carbon atoms. Compounds correlated with carbon like this are called with carbon compound or organic compounds. Carbon is very interesting element due to different forms according to bonding structure. Recently, lots of researchers have given an attention on interesting graphitic carbon forms such as fullerene, carbon nano tube and graphene. These different carbon forms are considered as one of nano materials of future technology for semiconductor and superconductor.

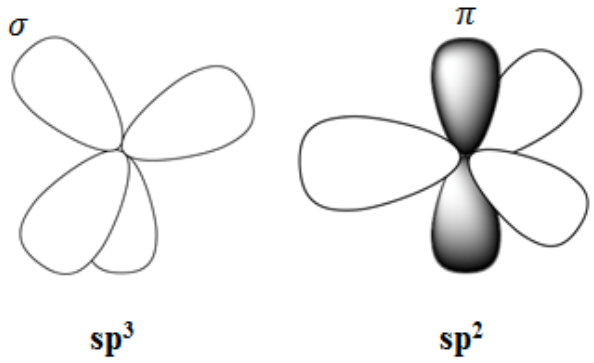

Fig. 1-2 Sp3 and sp2 hybridizing bonds

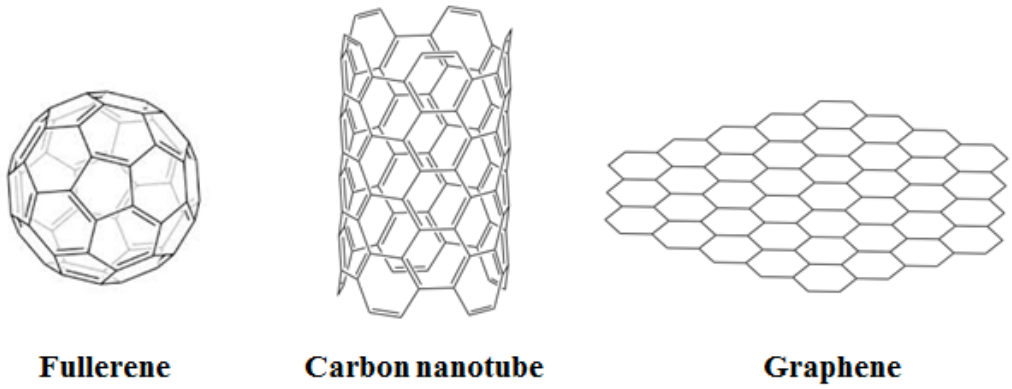

Fig. 1-3 Crystal structures of graphitic base carbon forms of fullerene, carbon nanotube and graphene

Graphene, that it is one of carbon allotropes, was suggested theoretically by P.R. Wallace in 1947. However, in 1930, Lev Landau and R.E. Peierls insisted that 2 dimensional crystalline could not exist with stable state because atoms of in it are thermally unstable. After that, N.D. Mermin made free-standing 2-D crystal structure but this structure could be temporarily exist, which experiment firmly supported theory of Landau-Peierls. By the way, in 2004, A.K. Geim succeeded to peel off graphene sheet from bulk graphite surface by using simple tape exfoliation [1], and then, properties and bandgap of graphene was evaluated. From this research, research of graphene has promoted to new era of carbon renaissance.

1.3 Graphene production method

1.3.1. *Top-down method*

- *Mechanical exfoliation from graphite*

After A.K. Geim and Novoselov[1] introduced graphene exfoliation technique form graphite in 2004, its superior properties like large specific surface area[2], superlative mechanical strength[3], superior transparency[4,5] and high thermal conductivity[6] has attracted intensively studies as an alternative material for high future society. After that, Philip Kim succeeded to extract graphene from graphite on tip of atomic force microscope (AFM) by using friction with surface of isolate material [7] in 2005.

Several graphite nanoplatelets had been produced from expanded graphite by using graphite intercalation method through fast vaporization of the intercalant at rising temperature. For instant, fast thermal enlargement from graphite with sulfuric acid intercalation, which is one of suitable treatments for producing nanoplatelets (or platelets). In addition, various expanded methods for graphite nanoplatelets such as ultrasound, exposure and ball milling and so on has been reported. [8-15]

GO (graphene oxide) has been obtained by the oxidation treatment from graphite, which are well known as methods of Staudenmeier [16], Hummers [17] and Brodie [18], respectively. Even after treatment, they showed a layered structure, however, their colors became lighter than that of graphite because of the much small amount of electronic conjugation oriented by the oxidation. As for the recent research [19–24], GO consisted of graphene oxide, which mainly had epoxyl and hydroxyl groups on their basal planes, and simultaneously carbonyl and carboxyl groups at the edges of their planes (Lerf–Klinowski model). These oxygen functional groups made layers of graphene oxide remain divided having hydrophilic properties at GO, so that, molecules of water could easily stay and intercalate between GO interlayers.

1.3.2. *Bottom-up method*

- *Large area deposition by chemical vapor deposition (CVD))*

BH Hong synthesized large area graphene through roll-to-roll method by using CVD method [25]. This graphene had superior properties of surface resistance of ~125 Ω/m^2 and optical transparent of 90 %. In detail, bi-layer graphene (BLG) was deposited on thin copper substrate. BLG is also very interesting topic, because different band structures can be obtained by controlling coupled stacking order between two single layer graphenes (SLGs) [26].

Table 1-1 Merits and challenges of conventional methods for graphene synthesis.

Properties	Method	Strong point	Weak point
Top-down	Mechanical exfoliation	High quality	Only for lab. Research, uncontrollable
	Mechanical milling	Mass production Simple setup	Contamination High defect
	Chemical exfoliation	Mass production Easy control	Contamination High defect
	Thermal expansion	High quality Mass production	Huge device High cost Difficult to control
Bottom-up	CVD	High quality Mass production	Huge device High cost Low energy efficiency

1.2.3. *Solution plasma process (SPP)*

- *Bottom-up SPP*

Recently, carbon materials have been synthesized by Solution Plasma Processing (SPP). SPP is a non-equilibrium, and cold plasma that induces extremely rapid reactions by the present of reactive chemical species, radicals, and UV radiation. For conventional plasma discharge in liquid, the precursor decomposes to carbon atoms due to high input energy and temperature, and then they progress to recombination and formation of carbon materials. On

the other hand, in solution plasma processing, the precursors are activated with keeping the molecular structure through C-H activation and react with other molecules because of low input energy and temperature, and then carbon materials are synthesized. Therefore, the properties of synthesized carbon materials depend on the original structure of the precursor. In other words, we can design the synthesized materials by the selection of the precursors.

By using SPP, synthesis of various materials such as carbon nano sphere (CNS), [27] graphene, [28] metal nano particle, [29-31] bimetallic nanoparticle, [32] non-metal catalyst, [33-35] mesoporous silica [36] and polymer [37] have been reported. Especially, CNS has attracted big attentions due to its application of Li-air battery with high capacity and durability. However, heat treatment was essential after CNS synthesis because of very low conductivity. [38]

- *Top-down SPP*

Generally, Van der Waals forces between graphite layers are weak and significantly smaller than that of covalent carbon-carbon chemical bonds in the planes. Thus for producing graphene from graphite, it is necessary to control the energy during the process so that the Van der Waals force between 002 plain of carbon layers is overcome, but the molecular structure consisting of the covalent C–C bonds remains intact. The energy of the conventional arc plasma exceeds the C–C bond energy and results in the destruction of both interlayer bonding and molecular structure of the graphite. Low-energy plasma in liquid phase may selectively overcome the Van der Waals force while maintaining the aromatic structure. Therefore well-controlled plasma in liquid may exfoliate graphene from graphite electrode without creating many defects in the structure. Through SPP, which has low-energy plasma in liquid was used for the graphite exfoliation.

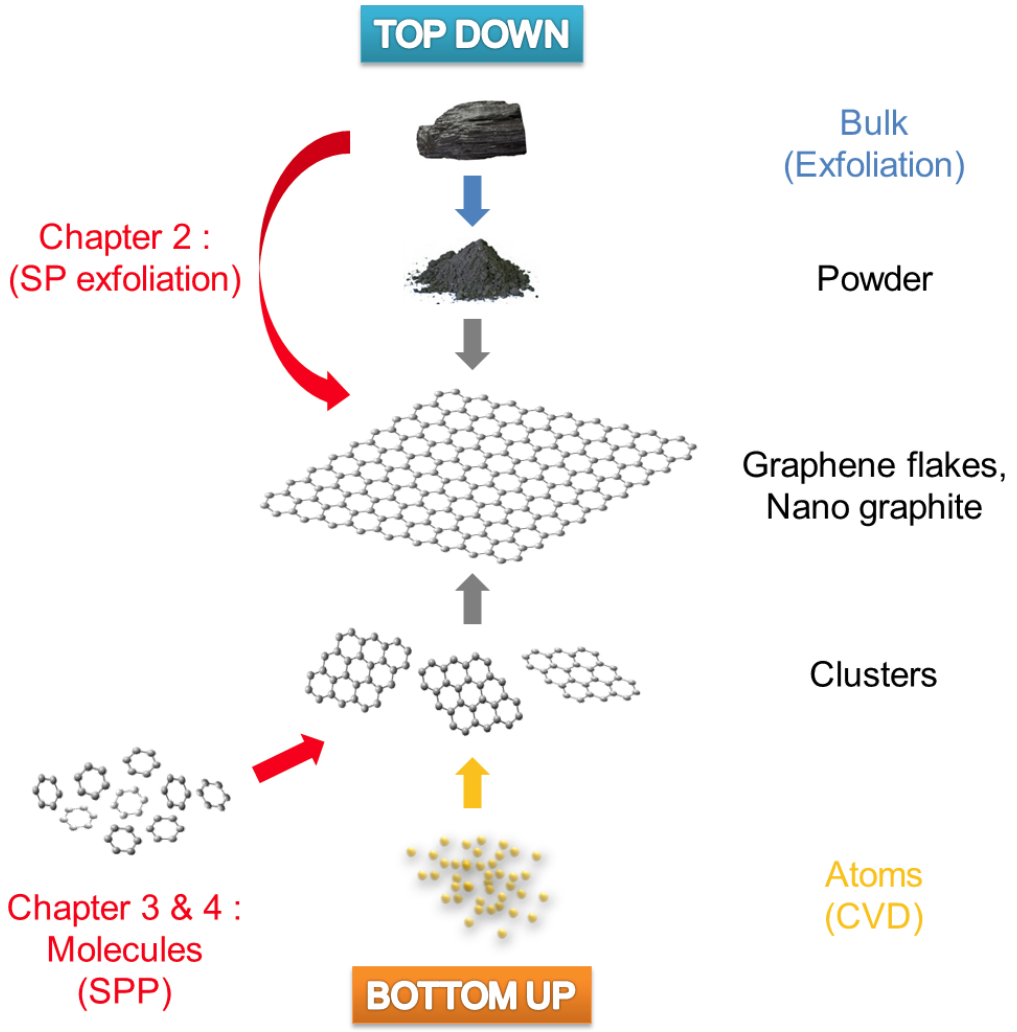

Fig 1-4 Approach for graphene nanoparticles construction

1.4 Application for electronics

Graphene is one single layer that carbon atoms are combined with honeycomb shape, which has high therma-electric conductivity, high strength, and flexibility. Application field of this graphene are energy, display, electronics like semiconductor, high efficiency solar cell, super capacitor, flexible display, smartphone, wearable computer, high strength composite materials and so on. Graphene is very versatile carbon structure for a wide application field like innovative display, solar energy and nano materials. Mass production technique is essential to progress on future society.

1.5 Object and outline of thesis

As mentioned in the previous section, mass production synthesis of graphene is very challenging for future society. In addition, structure control of carbon related with heterocarbon has been considered as essential studies for graphene related electronics and next generation batteries. Implantation of hetero element like N, B, S and P etc. at specific area could be realized with further understanding mechanism of carbon structure control as proceeding studies.

The purpose of this research is summarized in Fig. 1-4.

In chapter 2, graphene flakes was exfoliated from carbon electrode in water by SPP. The fundamental investigation of the temperature effect on the nanocarbon structure is discussed.

In chapter 3, conductive carbon with nano graphite structure was synthesized by using SPP in benzene. The effect of electrode gap on nanocarbon structure is discussed.

In chapter 4, improved conductive carbon with oriented graphite structure was synthesized by introducing solute in benzene. The effect of naphthalene and anthracene on nanocarbon structure, and mechanism of carbon formation during discharge are discussed.

Finally, chapter 5, summarized all of the chapters.

Table 1-1 Physical properties of graphitic-base carbon forms

properties	graphene	Carbon nanotube	Fullerene$_{60}$
structure	2-dimension(thickness : 0.34 nm)	1-demension (diameter : 1 nm~tens of nm length : 100 nm~1 cm)	0-dimension
Young modulus (Pa)	1T	~1.25 T (SWNT) 0.27~0.95 T (MWNT)	15.9 G
Tensile strength (Pa)	130 G	13~52 G (SWNT) 11~63 G (MWNT)	-
Bandgap (eV)	0 (zero-gap semimetal)	0~1.9 (conductor or semiconductor)	1.5~2.0 (*N*-type semiconductor)
Electric conductivity (S/cm)	~ $\times 10^5$	$0.17 \sim 2\times 10^5$	$10^{-14} \sim 6\times 10^{-8}$
Electron mobility (cm^2/Vs)	15,000 (electron, hole) At room temperature	1,000 (electron) ~4,000 (electron) At room temperature	0.5 ± 0.2 (electron) 1.7 ± 0.2 (electron) At room temperature
Thermal conductivity (W/mK)	2,000~5,000	6,600 (SWNT) 3,000 (MWNT)	0.4
Thermal stability (℃)	~2,800 (under Ar)	~1,800 (under Ar)	~1,000 (under Ar)
Solubility (g/mL)	4.1 ± 1.4 (DMF) 4.7 ± 1.9 (NMP)	23 ± 6 (DMF) 116 ± 10 (NMP)	27 (DMF) 890 (NMP)
Density (g/cm^3)	2.2	1.33	1.65

References

1) Novoselov, KS, Geim, AK., Morozov, SV, Jiang, D, Zhang, Y, Dubonos, SV, Grigorieva, IV, Firsov, AA, Science, 306, 666, 2004.
2) Stoller, MD, Park, SJ, Zhu, YW, An, JH, Ruoff, RS, Nano Lett., 8, 3498, 2008.
3) Lee C, Wei, XD, Kysar, JW, Hone J, Science, 321, 385, 2008.
4) Reina A, Jia X, Ho J, Nezich D, Son H, Bulovic V, Dresselhaus, MS, Kong J, Nano Lett., 9, 30, 2009.
5) Nair RR, Blake P, Grigorenko AN, Novoselov KS, Booth TJ, Stauber T, Peres NMR, Geim, AK, Science, 320, 1308, 2008.
6) Balandin AA, Ghosh S, Bao W, Calizo I, Teweldebrhan D, Miao F, Lau CN, Nano Lett., 8, 902, 2008.
7) Class of Physics, "Graphene" The royal Swedish Academy of Sciences, 2010.
8) Chen G, Weng W, Wu D, Wu C, Lu J, Wang P, et al., Carbon, 42, 753–9, 2004.
9) Chen G, Wu D, Weng W, Wu C, Carbon, 4, 619–21, 2003.
10) Weng W, Chen G, Wu D, Chen X, Lu J, Wang P, J. Polym. Sci., Part B: Polym. Phys., 42(15), 2844–56, 2004.
11) Chen G., Weng W., Wu D., Wu C., Eur. Polym. J., 39, 2329–35, 2003.
12) Kwon O., Choi S., Park K., Kwon Y., J. Ind. Eng. Chem., 2003, 9(6), 743–7.
13) Chen G, Wu C, Weng W, Wu D, Yan W, Polymer, 4, 1781–4, 2003.
14) Weng WG, Chen GH, Wu DJ, Yan WL, Compos. Inter., 11, 131–43, 2004.
15) Chen G, Wu D, Weng W, Yan W, Polym. Eng. Sci., 41, 2148–54, 2001.
16) Staudenmaier L, Ber. Dtsch. Chem. Ges., 31, 1481–99, 1898.
17) Hummers W., Offeman R., J. Am. Chem. Soc., 80, 1339, 1958.
18) Brodie BC, Ann. Chim. Phys., 59, 466–72, 1860.
19) Lerf A, He H, Forster M, Klinowski J, J. Phys. Chem. B, 102, 4477–82, 1998.
20) Lerf A, He H, Riedl T, Forster M, Klinowski J, Solid State Ionics, 101–103, 857–62, 1997.

21) He H, Riedl T, Lerf A, Klinowski J, J. Phys. Chem., 100, 19954–8, 1996.

22) Hontoria-Lucas C, Lopez-Peinado AJ, Lopez-Gonzalez JdD, Rojas-Cervantes ML, Martin-Aranda RM, Carbon, 33, 1585–92, 1995.

23) He H, Klinowski J, Forster M, Lerf A, Chem. Phys. Lett., 287, 53–6, 1998.

24) Szabo T, Berkesi O, Dekany I DRIFT, Carbon, 43, 3186–9, 2005.

25) Sukang Bae et al., Nature Nanotechnology 5, 574-578, 2010.

26) Zhiqiang Luo et al., "large-scale synthesis of bi-layer graphene in strongly coupled stacking order", Advanced Functional Materials, 21, 911-917, 2011.

27) OL Li, J Kang, K Urashima and N Saito, J. Inst. Electrostat. Jpn. 37, 22-27, 2013.

28) HS. Lee, MA Bratescu, T Ueno and N Saito, RSC Advances, DOI 10.1039/c4ra03253e, 2014.

29) MA Bratescu, SP Cho, O Takai and N Saito, J. Phys. Chem. C 115, 24569, 2011.

30) A Watanaphanit, G Panomsuwam and N Saito, RSC Advances, DOI 10.1039/c3ra45029e, 2013.

31) SP Cho, MA Bratescu, N Saito and O Takai, Nanotechnology 22, 455701, 2011.

32) J Kang and N Saito, RSC Advances, DOI 10.1039/c5ra04220h, 2015.

33) G Panomsuwan, N Saito and T Ishizaki, J. Mater. Chem. A, DOI 10.1039/c5ta00244c, 2015.

34) G Panomsuwan, N Saito and T Ishizaki, Phys. Chem. Chem. Phys. 17, 6227, 2015.

35) DW Kim, OL Li and N Saito, Phys. Chem. Chem. Phys., DOI 10.1039/c4cp03868a, 2014.

36) P Pootawang, N Saito, O Takai and SY Lee, Nanotechnology 23, 395602, 2012.

37) A Watanaphanit and N Saito, Polym, Degrad. Stab. 98, 1072-1080, 2013.

38) J Kang, OL Li and N Saito, Nanoscale 60, 292-298, 2013.

Chapter 2

Solution Plasma Exfoliation of Graphene Flakes from Graphite Electrodes

Chapter 2 - Solution Plasma Exfoliation of Graphene Flakes from Graphite Electrodes

2.1. Introduction

Graphene, an allotrope of carbon whose structure is a single planar sheet of carbon atoms arrayed in a honeycomb pattern, has attracted considerable interest from many researchers over the past decade. Since Novoselov et al [1]. have introduced graphene exfoliation techniqu e from graphite using a simple duct tape ('scotch tape' or 'peel-off' method) in 2004, its superior properties such as extremely high thermal conductivity [2], high transparency [3,4], large specific surface area [5] and high mechanical strength [6] have been intensively studied. Based on these properties, graphene is an alternative material for fuel cells, batteries, touch screens, transparent conductive films, high-frequency circuits, capacitors, removal materials, sensors, toxic- and flexible electronics. [4, 7-9]

In addition to the peel-off method, graphene was fabricated by chemical methods like chemical vapor deposition (CVD) and chemical exfoliation. The growth by CVD method provides graphene with excellent electronic conductivity although the method has the disadvantage of potential contamination on the surface by different organic compounds, which were commonly applied during the transfer on the target substrate. [10-13] Graphene fabricated by chemical exfoliation satisfies the cost and mass production requirements for industrial use, [14-16] especially in the application of printed electronic devices due to its stability in solution. [17,18] However, the material can barely be used in large area electronic panels and the conductivity is low compared to that of the CVD-graphene because many defects are produced during exfoliation process. [19]

Nanocarbon allotropes as nanofibers and multiple- or single tubes are usually synthesized

in low temperature plasma, plasma assisted CVD, and arc discharges. Plasma-assisted growth and production of graphene in recent years offer the possibility to synthesize graphene at lower temperatures. The use of plasma for graphene synthesis is quite challenging since it is very needed to both deliver tiny amounts of precursors, and enable fast and uniform nucleation, but avoiding any damage due to ion bombardment. [20, 21] Magnetically enhanced arc discharge has been used for the synthesis and separation of graphene flakes and single wall nanotubes during one-step process. [22]

Another important physical approach to synthesize nanocarbon allotropes is the application of electrical discharge in liquid where the carbon precursor can be either the electrode material or the liquid media. Carbon onions, [23] carbon nanohorns and nanotubes, [24-27] and metal nanoparticles covered by carbon [28, 29] were synthesized in plasma surrounded by a liquid.

Generally, Van der Waals forces between graphite layers are weak and significantly smaller than that of covalent carbon-carbon chemical bonds in the planes. Thus for producing graphene from graphite, it is necessary to control the energy during the process so that the Van der Waals force between the layers is overcome but the molecular structure consisting of the covalent C–C bonds remains intact. The energy of the conventional arc plasma exceeds the C–C bond energy and results in the destruction of both interlayer bonding and molecular structure of the graphite. Low-energy plasma in liquid phase may selectively overcome the Van der Waals force while maintaining the aromatic structure. Therefore well-controlled plasma in liquid may exfoliate graphene from graphite electrode without creating many defects in the structure. In this paper low-energy plasma in liquid termed solution plasma process (SPP) was used in order to execute the graphite exfoliation.

SPP is a non-equilibrium, cold plasma that induces extremely rapid reactions by the present of reactive chemical species, radicals, and UV radiation. SPP can be carried out at atmospheric pressure, within the glow discharge limits, and it permits a good level of control to be exerted over the chemical reactions. [30, 31] The process has been reported as an

innovative and simple method for the synthesis of various nanoscale materials. [32-36] In this study, low-energy plasma in the liquid phase is the most important characteristic that allow the synthesis of graphene flakes in water by the SPP exfoliation.

2.2. Experimental procedure

A schematic representation of the experimental setup is shown in Fig. 2-1. Graphite electrodes with purity of 99.9999% (Nilaco Co. Ltd.) were used as carbon precursor. The tips of the electrodes were cut in round-edge cone shape from 3 mm of the edge. The diameter of the electrodes was 3 mm and the inter-electrode gap was 0.5 mm. The discharge was performed in a beaker between two graphite electrodes using a bipolar pulsed power supply (MPS-R06K010-WP1-6CH; Kurita) operating at a voltage from 1 to 2 kV, a frequency from 10 to 60 kHz, and a pulse width from 1 to 4 μs, in distilled water with 0.06 μScm^{-1} conductivity. Due to aggregation, the samples (carbon materials) were resuspended in ethanol before carrying out the analysis.

The obtained nanocarbon materials were measured by Raman spectroscopy. The samples were prepared by blending with ethanol prior to drop on a silicon wafer. After the sample was dried, visible Raman spectroscopy was conducted at room temperature using a 532.5 nm laser (NRS-1000; JASCO). The laser power used for nanocarbon material analysis was 10 mW. Rayleigh scattering was eliminated by a notch filter with 100 cm^{-1} bandwidth. The Raman spectra were collected in different points within an area of about 1 mm^2.

The morphology and selected area electron diffraction (SAED) of the nanocarbon materials were witnessed by transmission electron microscopy (TEM) (JEM-2500SE, JEOL) with accelerated 200 kV. Samples for the TEM analysis were served after placing a drop of ethanol containing the carbon material on a Copper grid having holes in it. During TEM observation, the information of the suspended carbon materials on the edge of the amorphous carbon film from the Cu grid was carefully collected. The high resolution TEM (HRTEM)

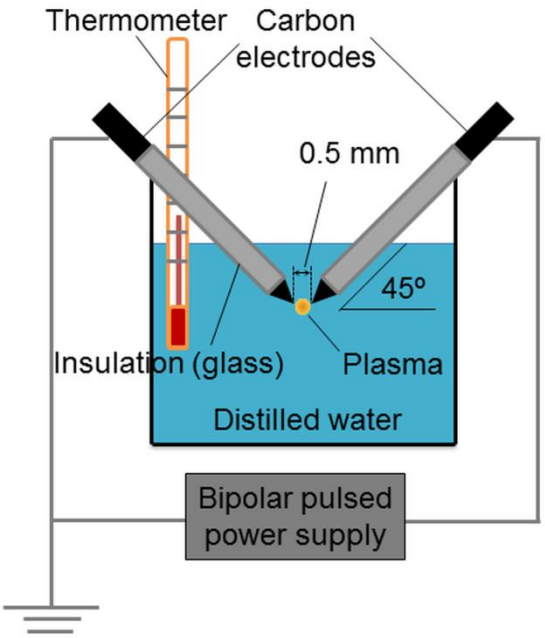

Fig. 2-1 Experimental setup for the solution plasma processing.

was executed by observing the objects near the Scherzer defocus. And then, the distance between lens and sample was controlled to sustain the objects focused within the optimum lens current. A beam current density for CCD camera observation of HRTEM was ~10 A cm^{-2}. At this time, temperature was elevated for a few degrees. This amount of beam current was studied to affect a little influence to the objects. [35] The differences between carbon structures were obtained from the electron energy loss spectroscopy (EELS) measurements of the carbon edge at 284 eV in HRTEM mode using a Gatan Imaging Filtering device. At this time, Digital Micrograph software was served with Filter Control. The EELS spectra were recorded with 2 mm aperture and 0.2 eV per pixel.

Time-averaged optical emission spectra (OES) of the discharge were observed with an optical spectrometer (HR2000+CG-UV-NIR; Ocean Optics) through a 5 mm diameter quartz window in the spectral range from 200 to 1100 nm and a resolution of 0.1 nm. [37] The discharge voltage and current were monitored using a high-voltage probe (P6015A; Tektronix) and a current probe (model 6595; Pearson Electronics), respectively, on an oscilloscope (DS1202CA; RIGOL). During the synthesis, the liquid temperature was measured with an alcohol thermometer.

2.3. Results and discussion

2.3.1 *Nanocarbon structure and morphology analysis*

Fig. 2-2 shows a schematic graph of the structural changes of the nanocarbon materials in dependence with the frequency and pulse width of the applied high voltage. Low energy discharges, which were generated at low frequency and low pulse width led to the formation of graphene flakes, whereas high energy discharges generated carbon onion structures. In the middle range, both graphene flakes and carbon onions were observed. Study on various methods of graphite exfoliation in liquid phase, for example, for graphene-ink preparation [38],

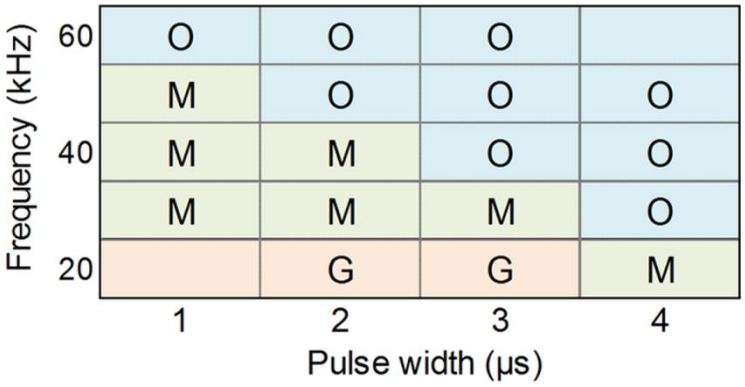

Fig. 2-2 Nanocarbon structural changes versus the experimental conditions measured from the waveforms of the bipolar pulsed power supply. The symbols are as follows: G: graphene flakes; O: onion structure; M: mixture of the carbon in both forms.

and dispersion of graphene in water-surfactant solutions [39] have shown that the defects in graphene sheets were related to the edges but not to the structural changes as occurs in the SPP.

Typical TEM, HRTEM and SAED images are shown in Fig. 2-3(a)–(f). Spherical carbon onions are shown in Fig. 2-3(a)–(c) and plain layered graphene flakes are shown in Fig. 2-3(d)–(f). The multiple nested onion-like particles displayed in Fig. 3(a) have diameters from 2 to 16 nm. In the case of graphene flakes, a large quantity was observed. However, most graphene flakes were disordered multilayers (see Figure S1 in supplementary information) [40]. Therefore, the estimation of the size distribution and number of layers in the flakes could not be conducted here. In Fig. 2-3(c), the diffraction image of the carbon onions looks like a ring pattern formed by many diffraction spots generated by different crystal orientations. In contrast, in Fig. 2-3(f), the diffraction pattern of a suspended graphene sheet shows distinct spots.

The EELS spectra of the carbon edge of the carbon onions and graphene flakes are correspondingly shown in Fig. 2-3(g) and (h). The excitation values of empty antibonding π^* and σ^* states in the carbon K-shell electron (1s) are ~285 eV and ~290 eV, respectively. In the case of the carbon onions the broad transition 1s-σ^* indicates a higher degree of disorder in this material than that of graphene flakes. The ratio between intensities of the absorption line 1s-π^* and 1s-σ^* (r) is related with the relative amount of sp^2 and sp^3 bonds in the material. **[41]** From EELS spectra, r ratio was found to be smaller in the case of the carbon onions than that of the graphene flakes, which indicates a higher disorder degree in carbon bonds.

Raman scattering, which is often used for monitoring the structural changes of carbon materials, provides additional information of the synthesized carbon in the SPP. Fig. 2-4(a), (b) and (c) show that both spherical carbon onions, graphene flakes and graphite electrode display three prominent peaks at ~1350 cm^{-1}, 1580 cm^{-1} and 2720 cm^{-1} known as D band, G band, and 2D band, respectively. [42, 43] In Fig. 2-4(a), the D band of carbon onions is wider

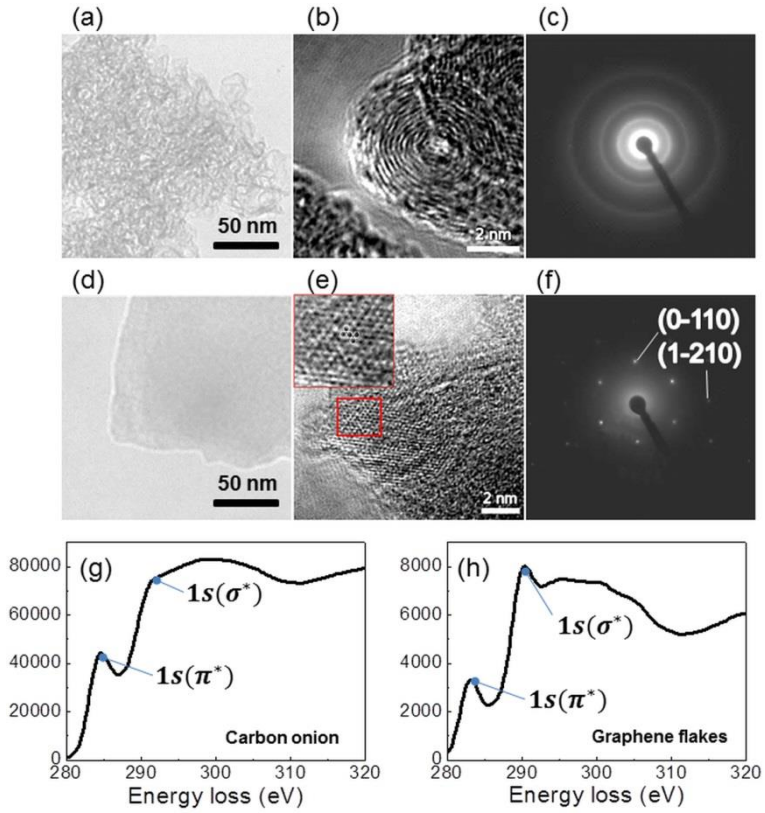

Fig. 2-3 Morphology images and diffraction patterns observed by TEM, HRTEM and SAED. (a) TEM image, (b) HRTEM image, and (c) SAED pattern of carbon onions synthesized at 60 kHz frequency and 2 μs pulse width and (d) TEM image, (e) HRTEM image, and (f) SAED pattern of graphene flakes obtained at 20 kHz frequency and 2 μs pulse width. Carbon edge of the EELS spectra corresponding to (g) carbon onions and (h) graphene flakes.

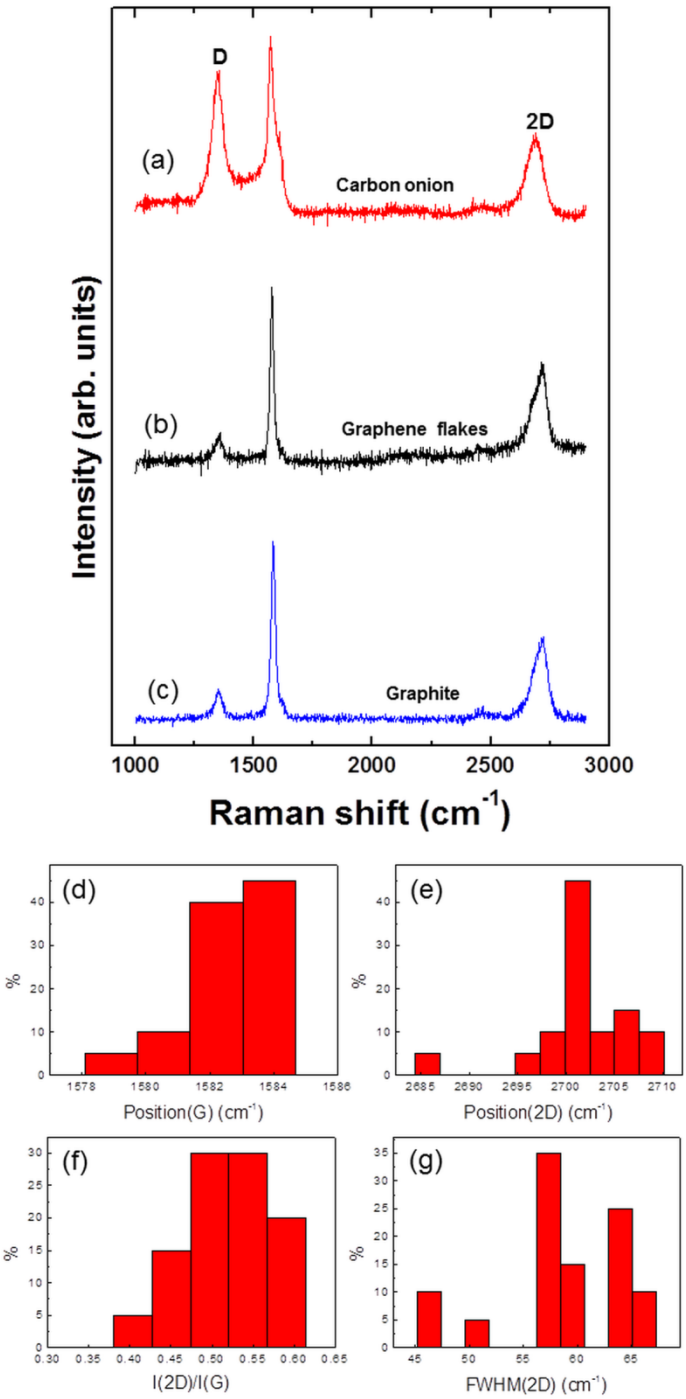

Fig. 2-4 Raman spectra of (a) carbon onion, (b) graphene flakes, and (c) graphite electrode on SiO_2/Si substrate measured a laser excitation wavelength at 532 nm. Statistical analysis of the Raman spectra of the graphene flakes within an area of about 1 mm^2 of (d) G band, (e) 2D band position, (f) ratio I_{2D}/I_G, and (g) FWHM of the 2D band. The *y*-axis in the plots (d)-(g) represents the percentage of the total number of measured spectra

and much higher than that of graphene flakes, which indicates that the carbon onions contain more disordered sp^2 carbon as well as defects. [43] The G band linewidth of the carbon onion is 58.6 cm^{-1}, which is wider than that of the graphene flakes where the value is 18.6 cm^{-1}. The spectrum of graphene flakes is similar to graphite electrode as presented in Fig. 2-4(c), which indicates that the graphene flakes were formed without destroying of carbon structure. The ratio between the intensities of D band (I_D) and G band (I_G) was additionally calculated. The I_D/I_G ratios in carbon onion and graphene flakes were 0.75 and 0.16, respectively. Due to the defects and disordered structure in carbon onion, the I_D/I_G ratio was higher. The distribution of the spectra collected within an area of about 1 mm^2 of graphene flakes is illustrated in Fig. 2-4(d)–(g). The analysis results showed that a precise control of the lateral sizes and the thickness of the graphene sheets cannot be obtained as was reported using a centrifugation procedure. [44, 45]

2.3.2 *Plasma composition and parameters*

Optical emission spectra and images of plasma during the synthesis of carbon onion and graphene flakes are shown in the Fig. 2-5(a) and (b), respectively. The synthesis of the carbon onions resulted in burning-like white colored plasma, accompanied with a lot of bursting bubbles and radiant heat which were detected nearby the experimental beaker. In contrast, purple colored-plasma and small amount of tiny bubbles were observed during the synthesis of graphene flakes.

In Fig. 2-5(a), the optical emission spectrum resembles typical arc plasma spectrum from blackbody radiation punctuated by the emission of many excited carbon species such as C_2, C, CO and CH at high relative intensity. A large amount of carbon was generated from an erosion of electrodes before reacting with H and O atoms produced from the water dissociation, and generating CO and CH radicals. In the case of the graphene flakes production (Fig. 2-5 (b)), the peak at 247.8 nm corresponding to the excited C atom radical

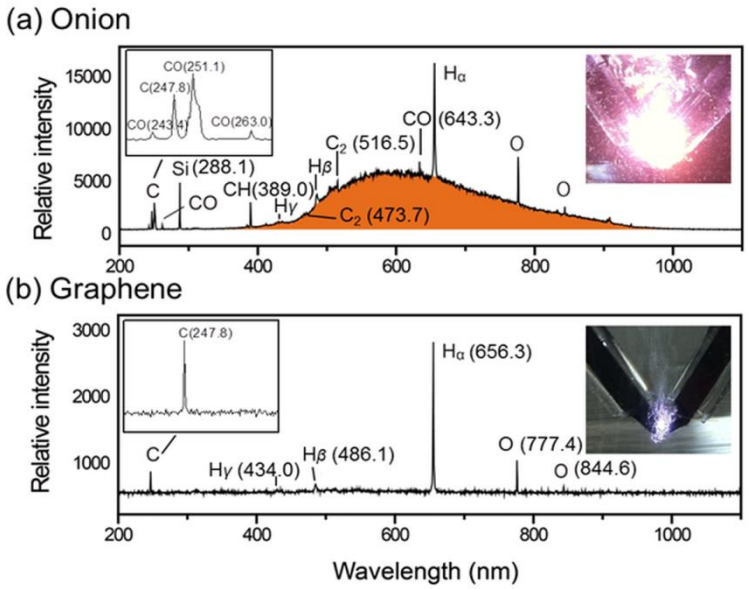

Fig. 2-5 Optical emission spectra and images of plasma generated during the synthesis of (a) carbon onion and (b) graphene flakes (Spectra identification is given in the Table S in the Supporting Information). On the right upper corners, images of plasma are inserted.

has a spectral intensity much lower than that of in the case of the carbon onions production. Other carbon radical peaks were not detected in the OES during the graphene flakes synthesis. The only observed radicals were H, O, and C atoms. The difference in the relative intensities indicated different contents of the gas bubbles surrounded by the solution and implied that gas bubbles formed during the synthesis of the carbon onions predominantly consist of carbon vapor, carbon monoxide, hydrogen and oxygen, whereas gas bubbles formed during the synthesis of the graphene flakes mainly consists of water vapor, small amount of hydrogen and oxygen gases, as well as carbon monoxide. The electron excitation energy was estimated from the ratio of hydrogen emission intensities of Hα and Hγ, at wavelengths of 656.3 and 434.0 nm, respectively, and was found to be 0.6 and 1.4 eV in the case of plasma used for the graphene flakes and carbon onions synthesis, respectively (Table 2-1).

From the spectrum shown in the Fig. 2-5(a), the temperature, *T*, of the electrode tip was calculated by using Wien's law:

$$\lambda_{\max} = \frac{2.898 \times 10^3}{T}$$

where $\lambda_{\max}$ is the wavelength corresponding to the maximum blackbody radiation distribution. In Fig. 2-5(a), $\lambda_{\max}$ is ~630 nm and *T* was calculated to be 4600 K, which is higher than the melting point (3825 K) and the boiling point (4489 K) of graphite. [46] The thermal energy of the gas in the vicinity of the electrode is 0.025 and 0.39 eV in plasma used for the graphene flakes and carbon onions synthesis, respectively. The surrounding water temperatures during the synthesis of carbon onions and graphene flakes were 373 K and 303 K, respectively (Table 2-1).

The input energy into plasma can be calculated using the current and voltage waveforms (see Figure S2 in the supplementary information) of the relation as shown below:

$$W = V \times I \times t$$

where *W*, *V*, *I* and *t* represents the energy, voltage, current and time, respectively. The calculated input energy per pulse in the case of the carbon onions formed at 60 kHz and 2 μs

Table 2-1 Parameters of plasma derived from the experimental data.

Parameter	Graphene flakes	Carbon onions
Electrode temperature *T*	300 K 0.025 eV	4600 K 0.39 eV
Electron excitation energy	6932 K 0.6 eV	16306 K 1.4 eV
Input energy in plasma	At 20 kHz and 2 μs 1.17×10^{-3} J	At 60 kHz and 2 μs 1.07×10^{-3} J
Power	14.1 W	82.6 W

was 1.07×10^{-3} J and in the case of the graphene flakes produced at 20 kHz and 2 μs was 1.17×10^{-3} J. For a fixed frequency, the values of energies per second were 82.6 and 14.1 W for the formation of the carbon onions and graphene flakes, respectively. Although the energy per pulse was almost the same, the input power considerably differed for different carbon structures. The higher energy per second, which resulted in carbon onions synthesis, can explain the Joule effect which determines the heating of the graphite tip electrode and the blackbody radiation.

2.3.3 *Synthesis mechanism*

Based on these results and calculations, a synthesis mechanism of nanocarbon materials can be developed. This is described in the following paragraphs and is summarized in Fig. 2-6.

2.3.3.1 *Plasma in water*

Mechanism of the bubbles formation is schematically represented in Fig. 2-6 (a). The initial input electrical energy is converted into thermal energy on the electrode surface, which heats water molecules and leads to vaporization. The gas bubbles nucleate at atmospheric pressure and plasma is generated inside the bubbles due to the high voltage applied between electrodes. Plasma is sustained and becomes stabilized under the bipolar pulsed voltage which generates a bipolar pulsed current. It is supposed that in the ionized gas a conduction channel is formed between electrodes by primary streamers.

In basic terms, the shape of plasma can be classified as corona discharge, glow discharge, spark discharge or arc discharge. In this experiment, spear-shaped electrodes were used, resulting in the plasma shape being very close to corona discharge with a high potential gradient. Nevertheless, the corona-shaped plasma was not dispersed and then streamers formed under atmospheric pressure due to high voltage and close inter-electrode gap in

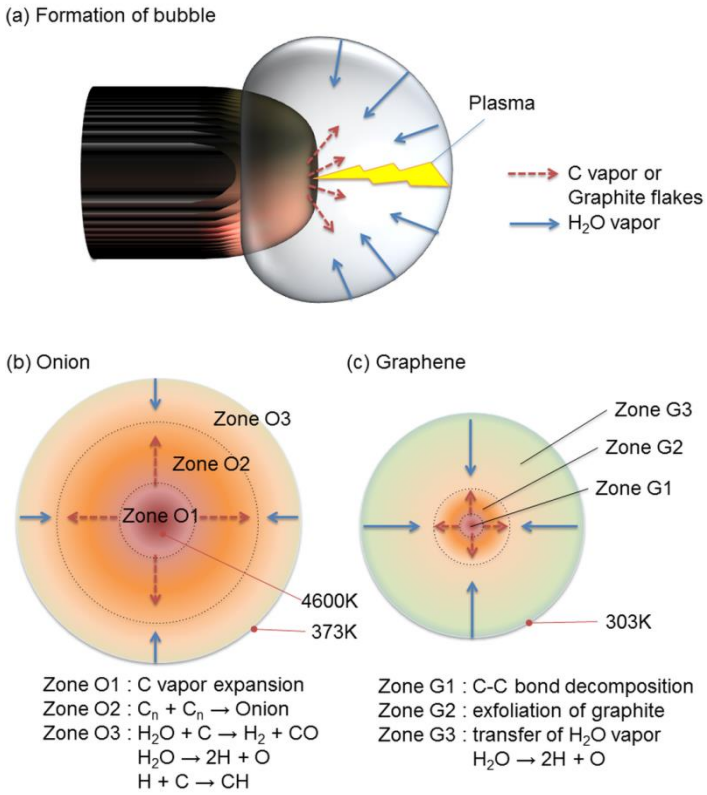

Fig. 2-6 (a) Proposed mechanisms for the bubble formation on the graphite electrodes discharged in distilled water. Reaction zones according to temperature distributions during the synthesis of (b) carbon onions and (c) graphene flakes.

relatively high molecular density. Plasma can hardly progress to arc discharge using the bipolar power supply because of the short discharge time determined by the pulse width from 1 to 4 μs, which created non-equilibrium plasma (i.e. the temperature of the electrons is much higher than that of the ions). Thus, in this experiment plasma starts from corona discharge at the beginning and progresses to spark discharge with an energy accumulation at the side. The streamers formed inside the bubbles between the immersed electrodes in water generate ions and radicals from atoms and molecules, which accelerate the chemical reactions.

In this plasma, the ions were not strictly thermal (meaning the gas temperature) since the electric field during the plasma operation was about 20 kV cm^{-1}, due to a mean free path less than 1 μm at atmospheric pressure, which could result in average energies for ions of about 1 eV. The average electron energy corresponding to this electric field is about 2 eV. [47]

2.3.3.2 *Carbon onions synthesis*

In the case of the synthesis of the carbon onions (Fig. 2-6 (b)), the measured temperature of the electrode tip was 4600 K, which is higher than the melting and boiling points of graphite. Therefore, in zone O1, graphite was vaporized and carbon atoms expand from the center of the bubble to the outer regions due to the higher temperature. A small fraction of carbon atoms were sputtered from the graphite electrode by fast ions from plasma. Zone O2 was the region where the carbon vapor quenches because of the temperature gradient. The expanding carbon atoms gradually lost their energy and recombined with each other. At this point, the final shape of the carbon atoms combined into spherical onion because of the low surface energy. Zone O3 is the region where the remaining carbon atoms come in contact with water vapor forming H_2 and CO. In plasma phase the fast electrons were responsible for the C–C bond dissociation which required 6.5 eV energy, atomic, and molecular excitation and ionization processes. [48]

2.3.3.3 *Graphene flakes synthesis*

Based on the study carried out by Schabel and Martins, the exfoliation energy of graphite sheets was less than 1 eV. [49] The ion energy around 1 eV was enough to produce graphite exfoliation [47]. In Fig. 2-6 (c), the gas bubbles for the graphene flakes formation were smaller and have a lower temperature than that of the carbon onions formation due to lower input power. During the graphene flakes formation, the dissociation of the C–C bond occurred in zone G1 on the electrode surface because of the focused plasma energy despite the smaller amount of carbon vapor and the lower vapor pressure compared with the onion case. In zone G2, the graphene flakes were exfoliated due to the temperature gradient on the electrode surface, which implied that the energy in the zone was not sufficient to break the covalent C–C bonds but was sufficient to overcome the Van der Waals forces and separate the graphene layers. Zone G3 is the region where water vapor was transported from the bubble surface to the bubble center and where H and OH radicals were generated from the dissociation of water molecules in plasma. Dissociation, ionization, and excitation processes were produced by the fast electrons present in the plasma gas phase. The necessary energy to get excited carbon atoms from the electrode was about 12.5 eV because the exfoliation process needed 1 eV, the dissociation of the C–C bond needed 6.5 eV, and the excitation of carbon atom from ground state $^1P^0$ to excited state ^1S (See supplementary information Table S) required about 5 eV. [50] Although the photon energy in the SPP can be about 5–6 eV, the photon flux was small and a photoexfoliation process of the graphite was negligible as compared with the exfoliation produced in plasma by ions and electrons.[51]

2.4. Summary

In summary, we have synthesized two different types of nanocarbon from graphite electrode: graphene flakes and carbon onions, by controlling the energy input from a bipolar

pulsed power supply during solution plasma process in water. The energy per pulse delivered in plasma was similar for both carbon onions and graphene flakes synthesis. However, the power delivered in plasma was much higher in the case of carbon onion synthesis. The main process to produce the carbon onions is carbon vaporization due to Joule effect and carbon recombination assisted by plasma. In order to produce graphene flakes, the graphite electrode was exfoliated in plasma. The diameter of the carbon onions was ranged from 2 to 16 nm and the graphene flakes were hundreds of nanometers in size. Unfortunately a precise control of the lateral sizes and the thickness of the graphene flakes was not realized. The HRTEM, TEM, and EELS analysis confirmed the morphology and the structure of the graphene flakes and carbon onions. The Raman spectra of the graphene flakes indicated that it was disordered multilayers.

References

1) KS Novoselov, AK Geim, SV Morozov, D Jiang, Y Zhang, SV Dubonos, IV Grigorieva and AA Firsov, 2004, *Science*, 306, 666-9.
2) AA Balandin, S Ghosh, W Bao, I Calizo, D Teweldebrhan, F Miao and CN Lau, 2008, *Nano Lett.*, 8, 902-7.
3) A Reina, X Jia, J Ho, D Nezich, H Son, V Bulovic, MS Dresselhaus and J Kong, 2009, *Nano Lett.*, 9, 30-5.
4) RR Nair, P Blake, AN Grigorenko, KS Novoselov, TJ Booth, T Stauber, NMR Peres and AK Geim, 2008, *Science*, 320, 1308.
5) MD Stoller, SJ Park, YW Zhu, JH An and RS Ruoff, 2008, *Nano Lett.*, 8, 3498-502.
6) C Lee, X Wei, JW Kysar and J Hone, 2008, *Science*, 321, 385-8.
7) R van Noorden, 2011, *Nature*, 469, 14-16.
8) V Chandra, J Park, Y Chun, JW Lee, IC Hwang and KS Kim, 2010, *ACS Nano*, 4, 3979-86.

9) WH Lee, J Park, Y Kim, KS Kim, BH Hong and K Cho, 2011, *Adv. Mater.*, 23, 3460-4.

10) KS Kim, Y Zhao, H Jang, SY Lee, JM Kim, KS Kim, JH Ahn, P Kim, JY Choi and BH Hong, 2009, *Nature*, 457, 706-10.

11) PW Sutter, JI Flege and EA Sutter, 2008, *Nat. Mater.*, 7, 406-11.

12) Z Sun, Z Yan, J Yao, E Beitler, Y Zhu and JM Tour, 2010, *Nature*, 468, 549-52.

13) X Li, W Cai, J An, S Kim, J Nah, D Yang, R Piner, A Velamakanni, I Jung, E Tutuc, SK Banerjee, L Colombo and RS Ruoff, 2009, *Science*, 324,1312-4.

14) YY Shao, J Wang, M Engelhard, CM Wang and YHJ Lin, 2010, *Mater. Chem.*, 20, 743-8.

15) YW Zhu, MD Stoller, WW Cai, A Velamakanni, RD Piner, D Chen and RS Ruoff, 2010, *ACS Nano*, 4, 1227-33.

16) G Williams, B Seger and PV Kamat, 2008, *ACS Nano*, 2, 1487-91.

17) L Grande, VT Chundi, Di Wei, C Bower, P Andrew and T Ryhanen, 2012, *Particuology*, 10, 1-8.

18) C Karuwan, C Sriprachuabwong, A Wisitsoraat, D Phokharatkul, P Sritongkham and A Tuantranont, 2012, *Sensors and Actuators B: Chem.*, 161, 549-555.

19) M Cheng, R Yang, L Zhang, Z Shi, W Yang, D Wang, G Xie, D Shi and G Zang, 2012, *Carbon*, 50, 2581-7.

20) G Nandamuri, S Roumimov and R Solanki, 2010, *Appl. Phys. Lett.*, 96, 154101.

21) K Ostrikov, EC Neyts and M Meyyappan, 2013, *Advances in Physics*, 62, 113.

22) O Volotskova, I Levchenko, A Shashurin, Y Raitses, K Ostrikovand and M Keidar, 2010, *Nanoscale*, 2, 2281.

23) N Sano, H Wang, I Alexandrou, M Chhowalla, KBK Teo and GAJ Amaratunga, 2002, *App. Phys.*, 92, 2783-8.

24) N Sano, 2005, *Carbon*, 43, 450-3.

25) N Sano, J Nakano and T Kanki, 2004, *Carbon*, 42, 686-8.

26) G Xing, S Jia and Z Shi, 2007, *Carbon*, 45, 2584-8.

27) MV Antisari, R Marazzi and R Krsmanovic, 2003, *Carbon*, 41, 2393-401.

28) C Poonjarernsilp, N Sano, T Charinpanitkul, H Mori, T Kikuchi and H Tamon, 2011, *Carbon*, 49, 4920-7.

29) H Lange, M Sioda, A Huczko, YQ Zhu, HW Kroto and DRM Walton, 2003, *Carbon*, 41, 1617-23.

30) J Hieda, N Saito and O Takai, 2008, *J. Vac. Sci. Technol. A*, 26, 854-6.

31) OL Li, J Kang, K Urashima and N Saito, 2013, *J. Inst. Electrostat. Jpn.*, 37, 22-27.

32) MA Bratescu, SP Cho, O Takai and N Saito, 2011, *J. Phys. Chem. C*, 115, 24569.

33) P Pootawang, N Saito, O Takai and SY Lee, 2012, *Nanotech.*, 23, 395602.

34) A Watanaphanit and N Saito, 2013, *Polym. Degrad. Stabil.*, 98, 1072-80.

35) SP Cho, MA Bratescu, N Saito and O Takai, 2011, *Nanotech.*, 22, 455701.

36) J Kang, OL Li and N Saito, 2013, *Nanoscale*, 60, 292-8.

37) C Miron, MA Bratescu, N Saito and O Takai, 2010, *Plasma Chem. Plasma Process.*, 30, 619-631.

38) F Torrisi, T Hasan, W Wu, Z Sun, A Lombardo, TS Kulmala, GW Hsieh, S Jung, F Bonaccorso, PJ Paul, D Chu, AC Ferrari, 2012, *ACS Nano*, 6, 2992-3006.

39) OM Marago, F Bonaccorso, R Saija, G Privitera, PG Gucciardi, MA Lati, G Calogero, PH Jones, F Borghese, P Denti, 2010, *ACS Nano*, 4, 7515-23.

40) M Lotya, Y Hernandez, PJ King, RJ Smith, V Nicolosi, LS Karlsson, FM Blighe, S De, ZM Wang, IT McGovern, GS Duesberg and JN Coleman, 2009, *J. Am. Chem. Soc.*, 131, 3611-20.

41) J Bruley, DB Williams, JJ Cuomo, DP Papas J., 1995, *Microscopy*, 180, 22.

42) AK Gupta, TJ Russin, HR Gutierrez and PC Eklud, 2009, *ACS Nano*, 3, 45-52.

43) AC Ferrari, FC Meyer, V Scardaci, C Casiraghi, M Lazzeri, F Mauri, S Piscanec, D Jiang, DS Novoselov, S Roth and AK Geim, 2006, *Phys. Rev. Lett.*, 97, 187401, 1-4.

44) AA Green, MC Hersam, 2009, *Nano Lett.*, 9, 4031-6.

45) F Bonaccorso, A Lombardo, T Hasan, Z Sun, L Colombo, AC Ferrari, 2012, *Materials Today*, 15, 564-89.

46) DR Lide. CRC handbook of chemistry and physics 90th edn. CD-ROM version; 2010.

47) NY Babaeva and MJ Kushner, 2011, *Plasma Sources Sci. Technol.*, 20, 035017.

48) Darwent B deB, 1970, *Bond Dissociation Energies in Simple Molecules*, NSRDS-NBS 31.

49) MC Schabel, JL Martins, 1992, *Phys. Rev. B*, 46, 7185.

50) http://physics.nist.gov/PhysRefData/ASD/lines_form.html Accessed 4 March 2014.

51) S Dhar, AR Barman, GX Ni, X Wang, XF Xu, Y Zheng, S Tripathy, Ariando, A Rusydi, KP Loh, M Rubhausen, AH C. Neto, B Zyilmaz, T Venkatesan, 2011, *AIP Adv.*, 1, 022109.

Supplementary information for HS Lee, MA Bratescu, T Ueno, N Saito

Solution plasma exfoliation of graphene flakes from graphite electrodes

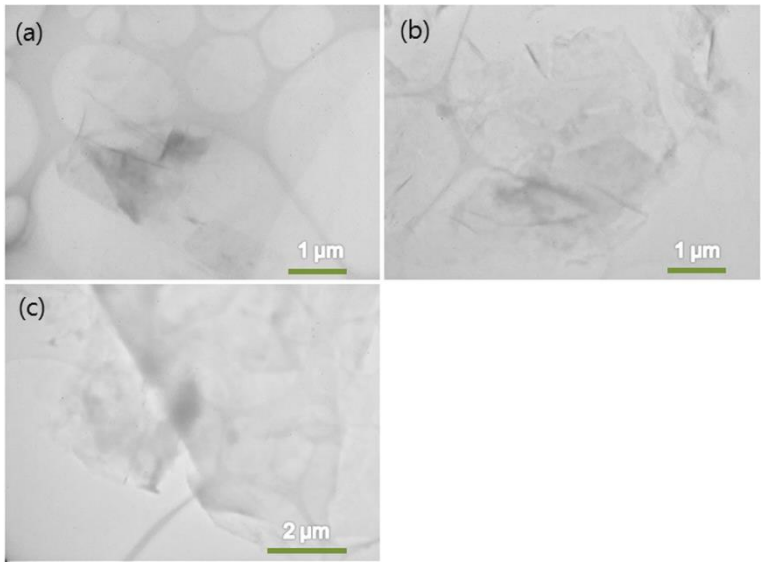

Figure 2-S1 Disordered multilayers images at low-magnification TEM observed in graphene flakes.

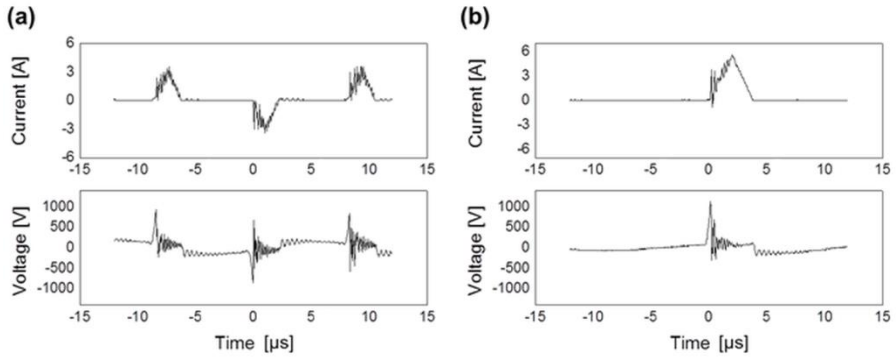

Figure 2-S2 Typical current and voltage waveforms during production of (a) carbon onions and (b) graphene flakes by solution plasma processing.

Table 2-S Identification of the excited species in OES [1S, 2S].

Species	λ (nm)	Transition
H_α	656.3	$3d \rightarrow 2p$
H_β	486.1	$4d \rightarrow 2p$
$H\gamma$	434.0	$5d \rightarrow 2p$
O	777.4	$^5P \rightarrow {}^5S^0$
	844.6	$^3P \rightarrow {}^3S^0$
C	247.8	$^1P^0 \rightarrow {}^1S$
Si	288.1	$^1P^0 \rightarrow {}^1D$
CH	389.0	$B^2\Sigma \rightarrow X^2\Pi$
CO	243.4	$A^1\Pi \rightarrow X^1\Sigma$
	251.1	$A^1\Pi \rightarrow X^1\Sigma$
	263.0	$A^1\Pi \rightarrow X^1\Sigma$
	643.3	$d^3\Delta \rightarrow a^3\Pi$
C_2	473.7	$A^3\Pi_g \rightarrow X'^3\Pi_u$
	516.5	$A^3\Pi_g \rightarrow X'^3\Pi_u$

[1S] Radzig AA, Smirnov BM, *Reference Data on Atoms, Molecules, and Ions*, Springer, 1985.

[2S] Pearse RWB and Gaydon AG 1976 *The Indentification of Molecular Spectra*, Chapman and Hall (London, New York)

Chapter 3

The Effect of Electrode Gap on Synthesis of Carbon Materials by Using Solution Plasma Process

Chapter 3 - The Effect of Electrode Gap on Synthesis of Carbon Materials by Using Solution Plasma Process

3.1. Introduction

Plasma discharge in liquid media has been used for synthesis of various carbon materials such as carbon onions, [1] carbon nanohorns and nanotubes, [2-5] metal particles covered by carbon, [6, 7] and metal catalyst in carbon matrix. [8]

Recently, carbon materials have been synthesized by Solution Plasma Processing (SPP). SPP is a non-equilibrium, and cold plasma that induces extremely rapid reactions by the present of UV radiation reactive, radicals and chemical species. For conventional plasma discharge in liquid, the precursor decomposes to carbon atoms due to high input energy and temperature, and then they progress to recombination and formation of carbon materials. On the other hand, in solution plasma processing, the precursors are activated with keeping the molecular structure through C-H activation and react with other molecules because of low input energy and temperature, and then carbon materials are synthesized. Therefore, the properties of synthesized carbon materials depend on the original structure of the precursor. In other words, we can design the synthesized materials by the selection of the precursors.

By using SPP, synthesis of various materials such as carbon nano sphere (CNS), [8] graphene, [9] metal nano particle, [10-12] bimetallic nanoparticle, [13] non-metal catalyst, [14-16] mesoporous silica [17] and polymer [18] have been reported. Especially, CNS has attracted big attentions due to its application of Li-air battery with high capacity and durability. However, heat treatment was essential after CNS synthesis because of very low conductivity. [19]

In this article, the effect of electrode distance on synthesized carbon materials has been investigated. Furthermore, crystallinity and resistance of carbon were controlled by setting up different electrode gap distance.

3.2. Experimental procedures

A schematic of the experimental setup is shown in Fig. 3-1. A total volume of 200 ml benzene was used as carbon precursor. Electric discharge was generated in a teflon reactor between high purity tungsten electrodes (99.999 %, Nilaco Co. Ltd.) by using a bipolar pulse power supply (MPP-HV02; KURITA) operated at a voltage between 1 kV and 2 kV, a frequency of 15 kHz, and a pulse width of 1.2 μs. The diameter of the electrodes was 0.8 mm. Effect of electrode gap distance on crystallinity of the synthesized carbon was studied by varying the inter-electrode gaps, before the discharge from 0.25 mm to 1 mm. The gap distance was subsequently measured after the discharge by using digital linear caliper (see Fig. S1). Note that the plasma discharge between electrodes of inter-electrode gap 1.25 mm was not feasible because the plasma was very unstable and hard to sustain its continuity. The carbon samples synthesized in the reactor with electrode gaps of 0.25, 0.5, 0.75, and 1 mm are hereafter designated as EG 0.25, EG 0.5, EG 0.75, and EG 1, respectively. Discharge at each condition was done for three times with a discharge time of 10 minutes. The obtained carbon powder was separated from the solution by filtering through the polytetrafluoroethylene (PTFE) membrane filter of 100 nm diameter before drying at room temperature in the air for an hour.

Morphology and electron diffraction pattern of the synthesized carbon materials were witnessed by transmission electron microscopy (TEM) (JEM-2500SE, JEOL) operating at an accelerating voltage of 200 kV. Samples for the TEM analysis were served by placing a drop of ethanol containing sample on Copper grid having holes in it prior to drying at room temperature. During TEM observation, information of the suspended carbon materials on the edge of the amorphous carbon film from the Cu grid was carefully collected. Chemical composition of the sample, including hydrogen, nitrogen, and carbon was measured by

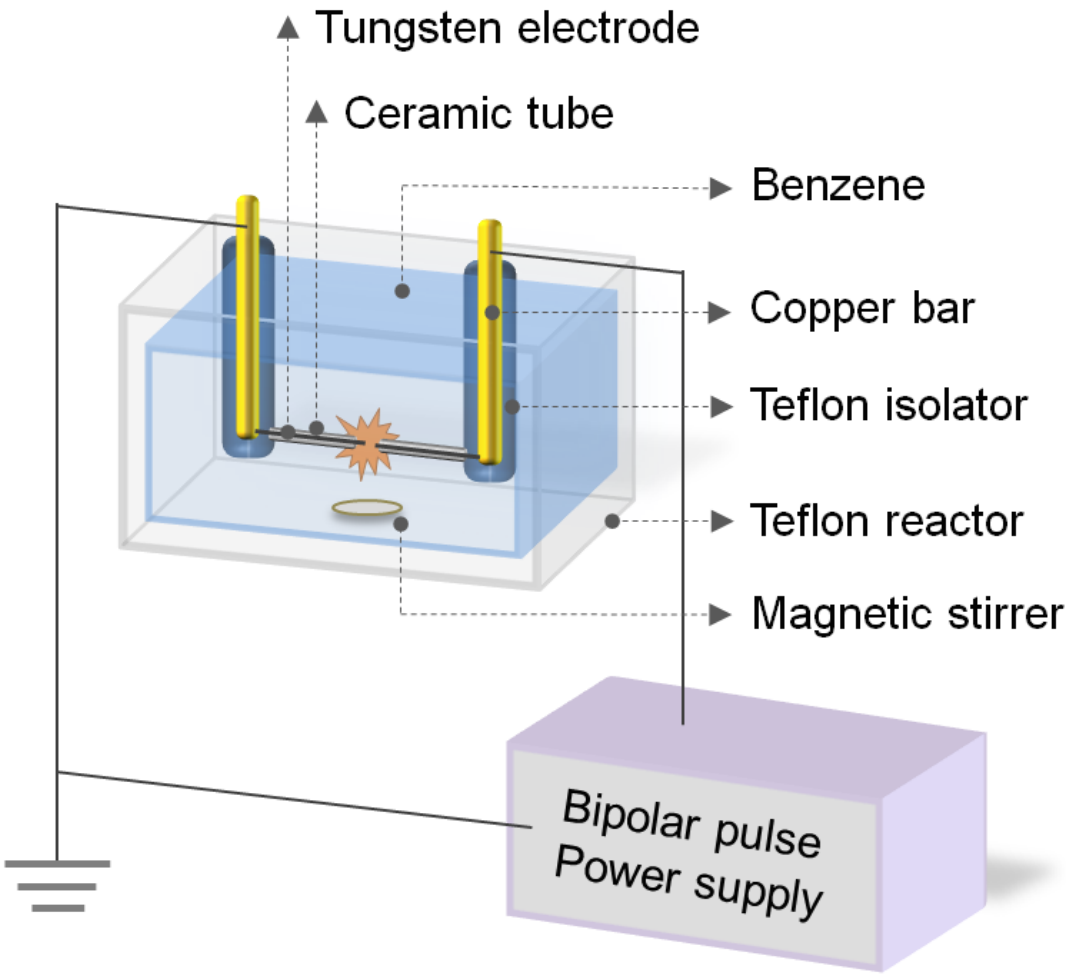

Fig. 3-1 Experimental setup for the solution plasma processing.

elemental analysis (MT-6; YANACO). Resistance of the carbon powder was calculated from data collected by using ohm meter (2001 multimeter; TFF Corp. Keithley Instruments) and DC constant power supply (model 692A; Metronix Corp.). Each sample was placed in a hollow teflon cylinder (inner diameter = 5 mm), and compressed in air between two commercial brass pistons forming the electrodes, the upper one movable and the lower one fixed. Obtained carbon powder were inserted into the cylinder and pressed between pistons. The load of pressure on the pistons was ~600 kPa by using a hand oil-pressure pump. Fundamental characteristics (discharge voltage and current) were measured by a digital oscilloscope (TDS 3014B; Tektronix) via high voltage and current probe.

3.3. Results and discussion

3.3.1 Conductivity and crystallinity of carbon

The conductivity of as-prepared carbon increased with increasing inter electrode gap, which is corresponding to C-C sp^2 bonding. Thus, the conductivity/resistivity can serve as the evaluation parameter of the degree of crystallinity in carbon. Fig. 3-2 showed the resistance of the as-prepared carbon samples. The resistance dropped linearly from 19k Ω·cm at EG 0.25 to 47 Ω·cm at EG 1. The values of electrode gaps were rearranged with average value before and after experiments. On average, the erosion rate of EG 0.25, EG 0.5, EG 0.75and EG 1 after 10 minute discharge were 0.09 mm (± 0.03), 0.08 mm (± 0.03), 0.03 mm (± 0.04) and − 0.05 mm (± 0.05), respectively. This result was connected with sharp peak intensity change of WC_{1-x}, those were plains of 111, 200, 220 and 311 at 36.7, 42.4, 61.8 and 74.2, at X-ray diffraction (XRD) (see Fig. 3-S2). However, it was not easy to distinguish broad carbon peak differences among samples, which were plains of 001, 002 and 100/101 at 12.3, 23.4 and 43, respectively.

The reduction of resistance was consistent with the results from elementary analysis. In Fig. 3-3(a), the H/C ratio of as-prepared carbon decreased with increasing electrode gap from the

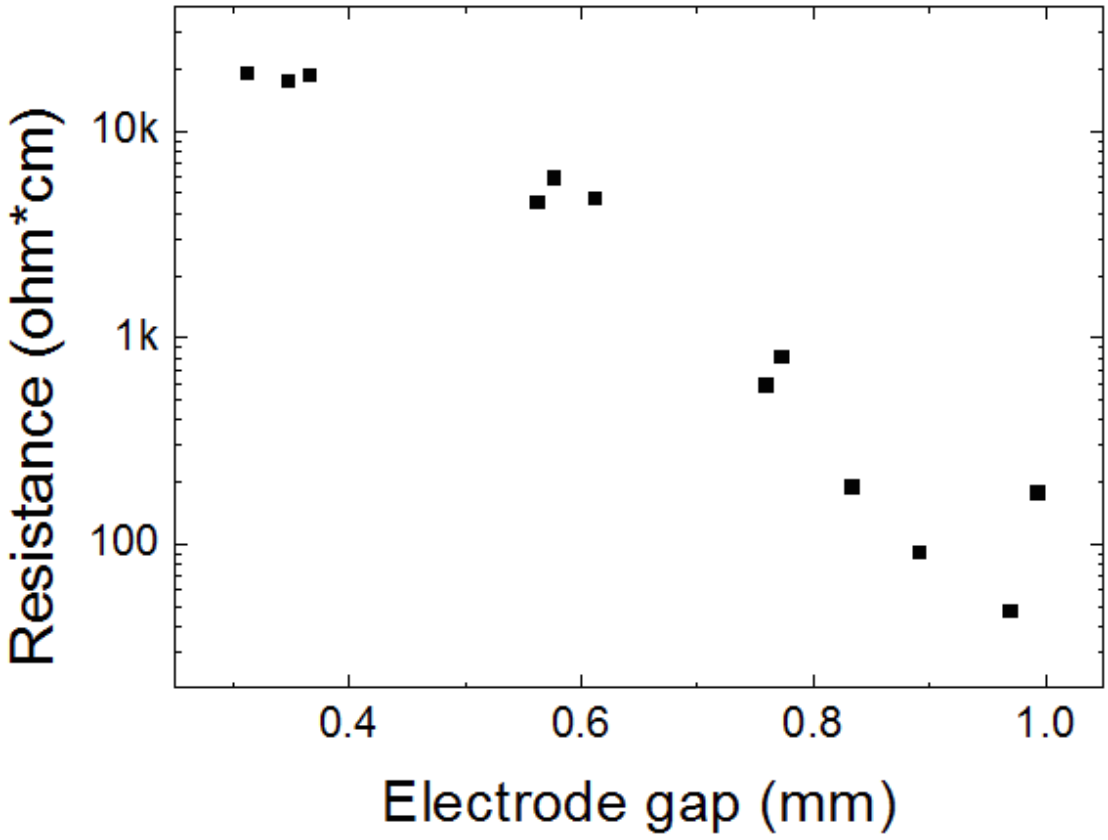

Fig. 3-2 Resistances of carbon powders according to inter electrode gap distance were measured by 4 probe measurement. The values of electrode gaps were rearranged with average value before and after experiments.

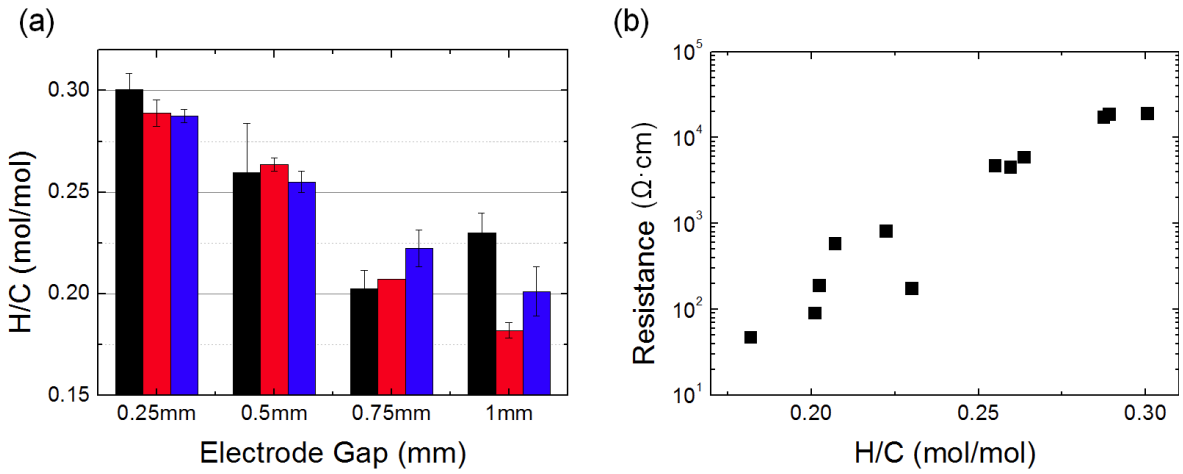

Fig. 3-3 (a) H/C ratio of as-prepared carbon powders measured from inter-electrode gap differences of 0.25 mm, 0.5 mm, 0.75 mm and 1 mm. (b) H/C ratio also was shown related with resistance value of each one.

value of 0.31 to that of 0.18. If you see Fig. 3-3(b), it is further clear that the H/C ratio decreased with decreasing the value of resistance. Since the sp3 bonding between H and C atoms has a negative effect on crystallinity, the resistance was also highly affected by the H/C ratio. It was supposed that tungsten metal particles had not that much effect on electric conductivity because conductivity of EG 0.25 showed the highest value despite it had lots of tungsten particles.

Typical TEM and selected area electron diffraction (SAED) images are shown in the Fig. 3-4. A low magnification TEM investigation of all samples like Fig. 3-4(a) and (b) showed that the shape of carbons are CNS, which have chain-like orbicular structure with comparably consistent size and their composition group is looked like carbon black. The mean diameter or diameter of gyration of all CNSs was estimated to be 20 to 30 nm. However, a high magnification TEM showed that obtained carbon of EG 0.25 at Fig. 3-4(c) was almost amorphous structure while the carbon of EG 1 at Fig. 3-4(d) showed the formation of crystalline graphite layers. This formation is supposed to be turbostratic structure in which graphite layers are oriented parallel to the concentric direction. Tungsten nano particles in EG 0.25 were sometimes observed, which were spread partially inside carbon and average size of them were estimated 5~7 nm. The other hand, tungsten nano particles in EG 1 were rarely observed. The SAED images showed similar ring patterns of graphitic carbon, that is to say, the plain of 002, 100 and 101 from the center to outer order. The pattern intensity of each plain of EG 1 was clearly observed stronger than that of EG 0.25.

3.3.2 Characteristics of solution plasma process

The voltage and current waveforms and images during discharge of inter-electrode gap 0.25 mm and 1 mm in benzene are shown in Fig. 5a and b, respectively. The high pulse voltage in benzene solvent generated the breakdown in it and free electrons were accelerated in the plasma gas phase. The streamers formed inside the bubbles between the immersed electrodes in water generate ions and radicals from atoms and molecules, which accelerate the chemical

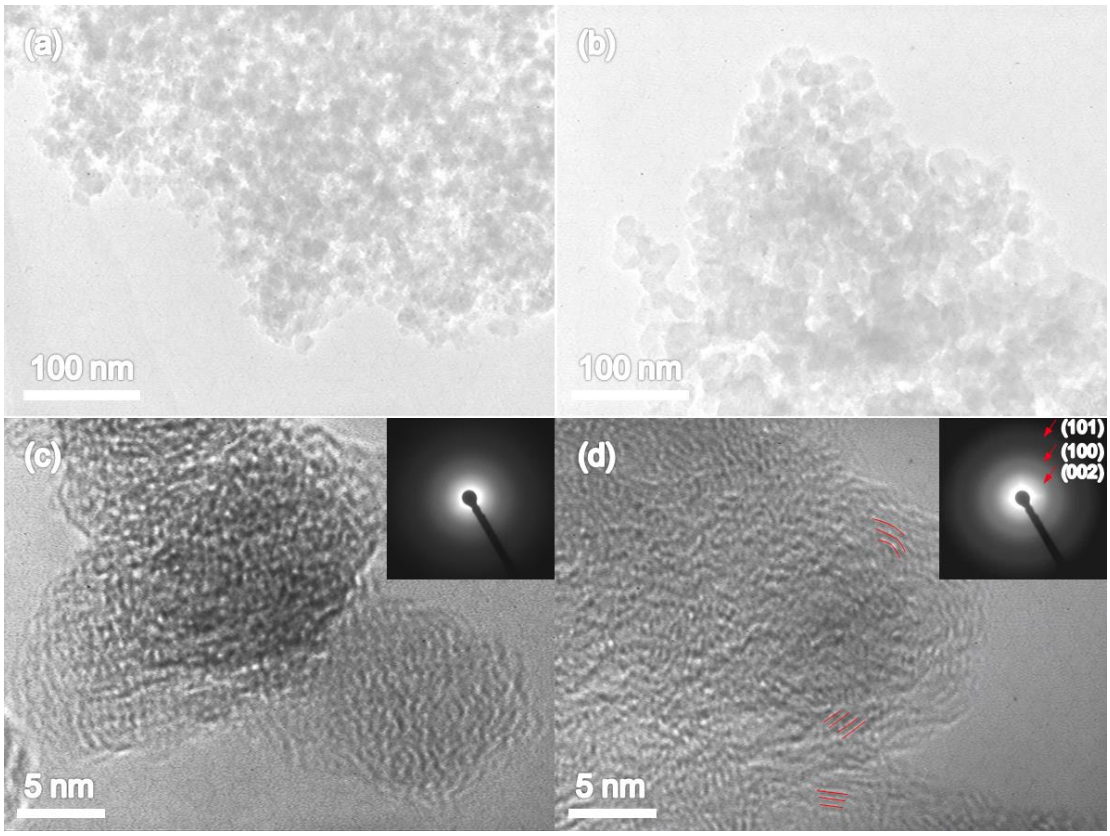

Fig. 3-4 Morphology images and diffraction patterns observed by TEM and SAED. (a), (b) TEM and (c), (d) SAED pattern of EG 0.25 and EG 1. Resistance value of EG 0.25 and EG 1 was 19k Ω·cm and 47 Ω·cm, respectively.

reactions. The energy input per pulse is calculated by $E = \int_0^t VI\,dt$ where E represents the energy (J per pulse), t, V and I represent the pulse width, voltage and current, respectively. It is confirmed that the energy per pulse during the carbon synthesis of EG 0.25 and EG 1 are 166 and 211 μJ, respectively. The current and voltage waveforms during production of carbon by solution plasma process were measured with almost same shapes as shown in Fig. 3-5(a)−(b). However, the intensity of each current peak of electrode gap 1 mm was lower than that of electrode gap 0.25 mm as shown in Fig. 3-5(c) −(d). This could be explained by the equation of V = IR where V represents the voltage, I and R represent the current and resistance, respectively. The value of R in plasma circuit could be high with increase of electrode gap distance, which made intensity of I decrease, apparently. From both discharge images, producing carbon density of electrode gap 1 mm was thicker than that of electrode gap 0.25 mm, while distribution of bubbles from center of discharge was narrower than that of electrode gap 0.25 mm. On average, the amount of obtained EG 0.25, EG 0.5, EG 0.75 and EG 1 were 2.4, 4.5, 6.2 and 4.5 mg/min, respectively.

3.3.3 Discussion

Resistance of obtained carbon material and H/C ratio decreased according to increase of electrode gap distance. If it was assumed that defects by hydrogen atoms and sp^3 carbon domains were obstacles of electron currency, decrease of resistance should be resulted by increase of sp^2 carbon domain in quantity or size. However, it was not very clear whether quantity of sp^2 domain increased or not at the result of raman spectra (see Fig. 3-S3). Therefore, we focused on the size of sp^2 carbon domain. For deeper understanding relation of H/C ratio and size in sp^2 domain, several equations and figure were proposed as followed (Eq. (1)-(3) and Fig. 3-6).

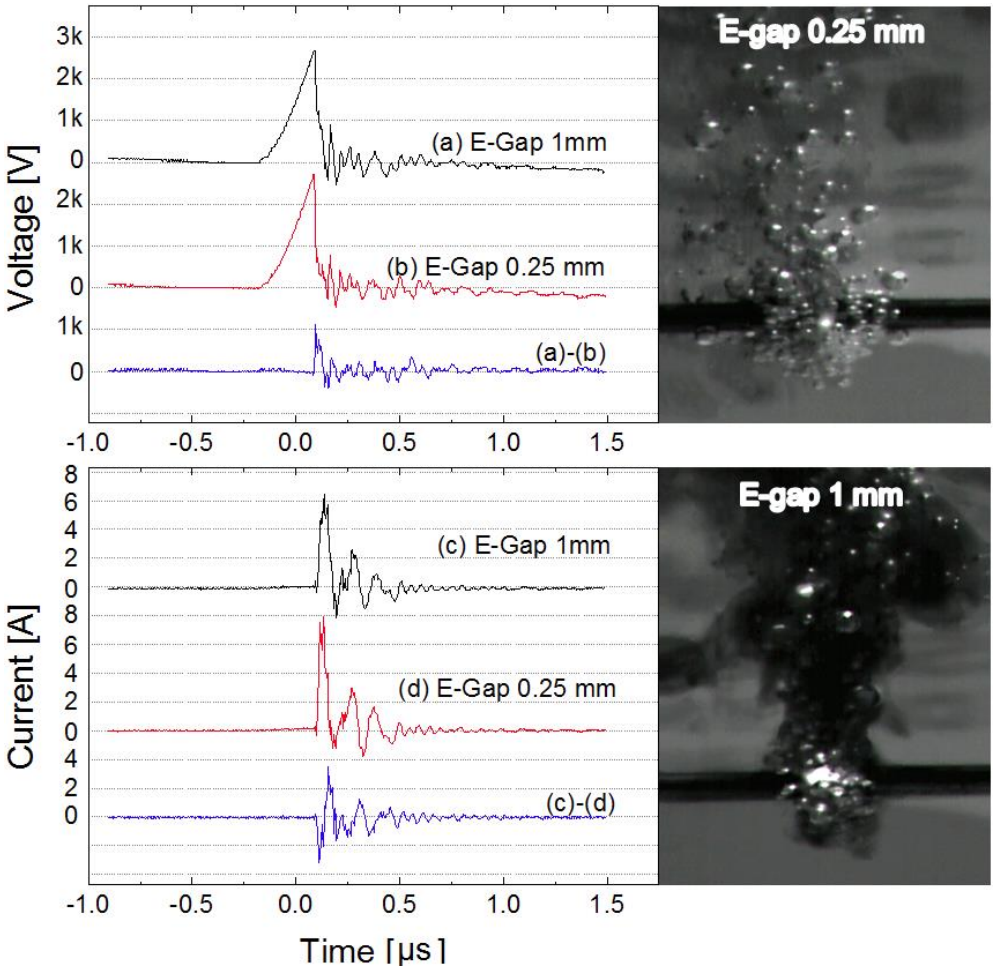

Fig. 3-5 Current and voltage waveforms during production of carbon nanospheres (CNSs) at different inter electrode gap of 0.25 mm and 0.1 mm by solution plasma processing. On the right side comers, images of plasma, bubbles and carbon production in benzene during electric discharge by using high speed camera are shown.

$$C_n = 6 + \sum_{k=1}^{n}\{8(2k-1)\} = 8n^2 - 2 \qquad (n \geq 1) \qquad (1)$$

$$H_n = 8n - 2 \qquad (n \geq 1) \qquad (2)$$

$$\frac{H_n}{C_n} = \frac{4n-1}{4n^2-1} \qquad (n \geq 1) \qquad (3)$$

Where Cn and Hn represent the number of hydrogen and carbon in 2-dimensional sp^2 structure, respectively. Calculated values of Cn, Hn and H/C were presented in table 3-1. The values of H/C ratio in EG 0.25 and EG 1 were 0.31 and 0.18, respectively. This means that n change from 3 to 5. The width between carbon 1 and opposite carbon 4, and the height between carbon 2 and 6 in benzene ring structure (Fig. 3-6(b)) are about 0.284 nm and 0.246 nm, respectively. Consequently, size of sp2 carbon structure can be calculated by Eq. (4) and (5).

$$L = 2a + (n-1) \times 6a = (6n-4) \times a \qquad (a = 0.142) \qquad (4)$$

$$I = (2n-1) \times b \qquad (b = 0.246) \qquad (5)$$

Where L, I, a and b represent the distance of horizontal axis, that of vertical axis, half value of width in benzene ring structure and the height of benzene ring structure, respectively(Fig. 3-6(b)). From the Eq. (4) and (5), the size of sp^2 carbon structure in EG 1 was 3.3 times larger than that of EG 0.25. Large size's sp^2 carbon structure is supposed to easy to aggregate together layer by layer due to accumulated large π bonding force. Based on the study carried out by Schabel and Marins, the interplanar binding energy of graphite was 25 meV per atom20. The average value of accumulated π bonding force in EG 1 was 4.95 eV, which is approximately 14 times larger than that of EG 0.25 at the value of about 0.35 eV.

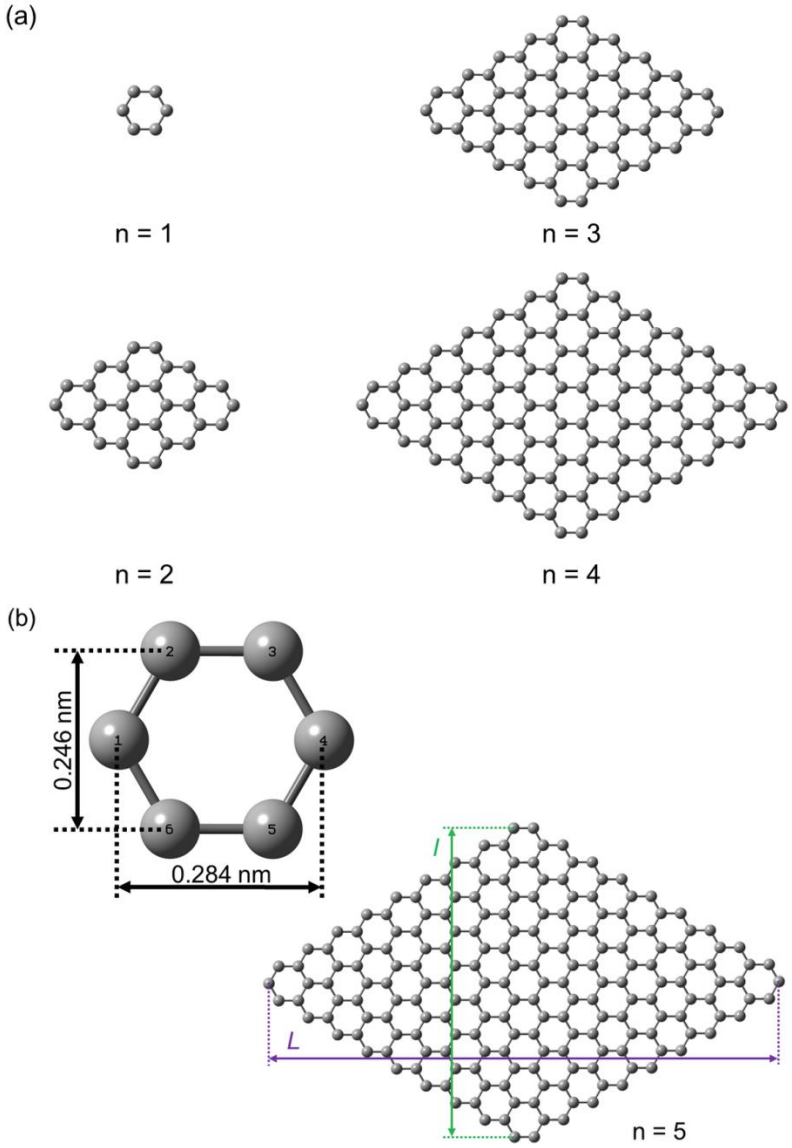

Fig. 3-6 Schematic representation of (a)size differences with the number of *n* change in the sp^2 carbon structure. Size of (b)benzene ring structure and sp2 carbon.

Table 3-1 Calculated H/C ratio with size differences in sp2 carbon domain.

n	***Cn***	***Hn***	**H/C**
1	6	6	1.000
2	30	14	0.467
3	70	22	0.314
4	126	30	0.238
5	198	38	0.192
6	286	46	0.161
7	390	54	0.138
8	510	62	0.122
9	646	70	0.108
10	789	78	0.098
11	966	86	0.089
12	1150	94	0.082
13	1350	102	0.076
14	1566	110	0.070
15	1798	118	0.066

3.4. Summary

Graphitic carbon structure was synthesized from benzene solvent by using solution plasma process and controlled through adjusting electrode gap distances. This effect plays the essential role as a main element at discharge process in organic solvent. TEM and diffraction images of EG 1 showed ordered graphitic layers and clear ring pattern compared with EG 0.25. The only adjustment of electrode gap distance from 0.25 mm to 1 mm had brought about approximately 400 times improvement of conductive property from 19k Ω·cm to 47 Ω·cm. From the result of CHN elemental analysis, H/C ratio decreased with decrease of resistance from 0.31 to 0.18. The increase of sp^2 carbon domains in size may cause to improvement of conductivity.

References

1) N Sano, H Wang, I Alexandrou, M Chhowalla, KBK Teo and GAJ Amaratunga, J. Appl. Phys. **53**, 113 (2013).
2) N Sano, Carbon **43**, 450-453 (2005).
3) MV Antisari, R Marazzi and R Krsmanovic, Carbon **41**, 2393-2401 (2003).
4) T Takenouchi, *Handotai* (Semiconductors) (Shokabo, Tokyo, 1964) p.83 [in Japanese].
5) N Sano, J Nakano and T Kanki, Carbon **42**, 686-688 (2004).
6) G Xing, S Jia and Z Shi, Carbon **45**, 2584-2588 (2007).
7) C Poonjarernsilp, N Sano, T Charinpanitkul, H Mori, T Kikuchi and H Tamon, Carbon **49**, 4920-4927 (2011).
8) H Lange, M Sioda, A Huczko, YQ Zhu, HW Kroto and DRM Walton, Carbon **41**, 1617-1623 (2003).
9) OL Li, J Kang, K Urashima and N Saito, J. Inst. Electrostat. Jpn. **37**, 22-27 (2013).

10) HS Lee, MA Bratescu, T Ueno and N Saito, RSC Advances, DOI 10.1039/c4ra03253e (2014).

11) SP Cho, MA Bratescu, N Saito and O Takai, Nanotechnology **22**, 455701 (2011).

12) MA Bratescu, SP Cho, O Takai and N Saito, J. Phys. Chem. C **115**, 24569 (2011).

13) A Watanaphanit, G Panomsuwam and N Saito, RSC Advances, DOI 10.1039/c3ra45029e (2013).

14) J Kang and N Saito, RSC Advances, DOI 10.1039/c5ra04220h (2015).

15) G Panomsuwan, N Saito and T Ishizaki, J. Mater. Chem. A, DOI 10.1039/c5ta00244c (2015).

16) G Panomsuwan, N Saito and T Ishizaki, Phys. Chem. Chem. Phys. **17**, 6227 (2015).

17) DW Kim, OL Li and N Saito, Phys. Chem. Chem. Phys., DOI 10.1039/c4cp03868a (2014).

18) P Pootawang, N Saito, O Takai and SY Lee, Nanotechnology **23**, 395602 (2012).

19) A Watanaphanit and N Saito, Polym, Degrad. Stab. **98**, 1072-1080 (2013).

20) J Kang, OL Li and N Saito, Nanoscale **60**, 292-298 (2013).

21) MC Schabel and JL Martins, PPhys. Rev. B: Condens. Matter Mater. Phys. **46**, 7185 (1992).

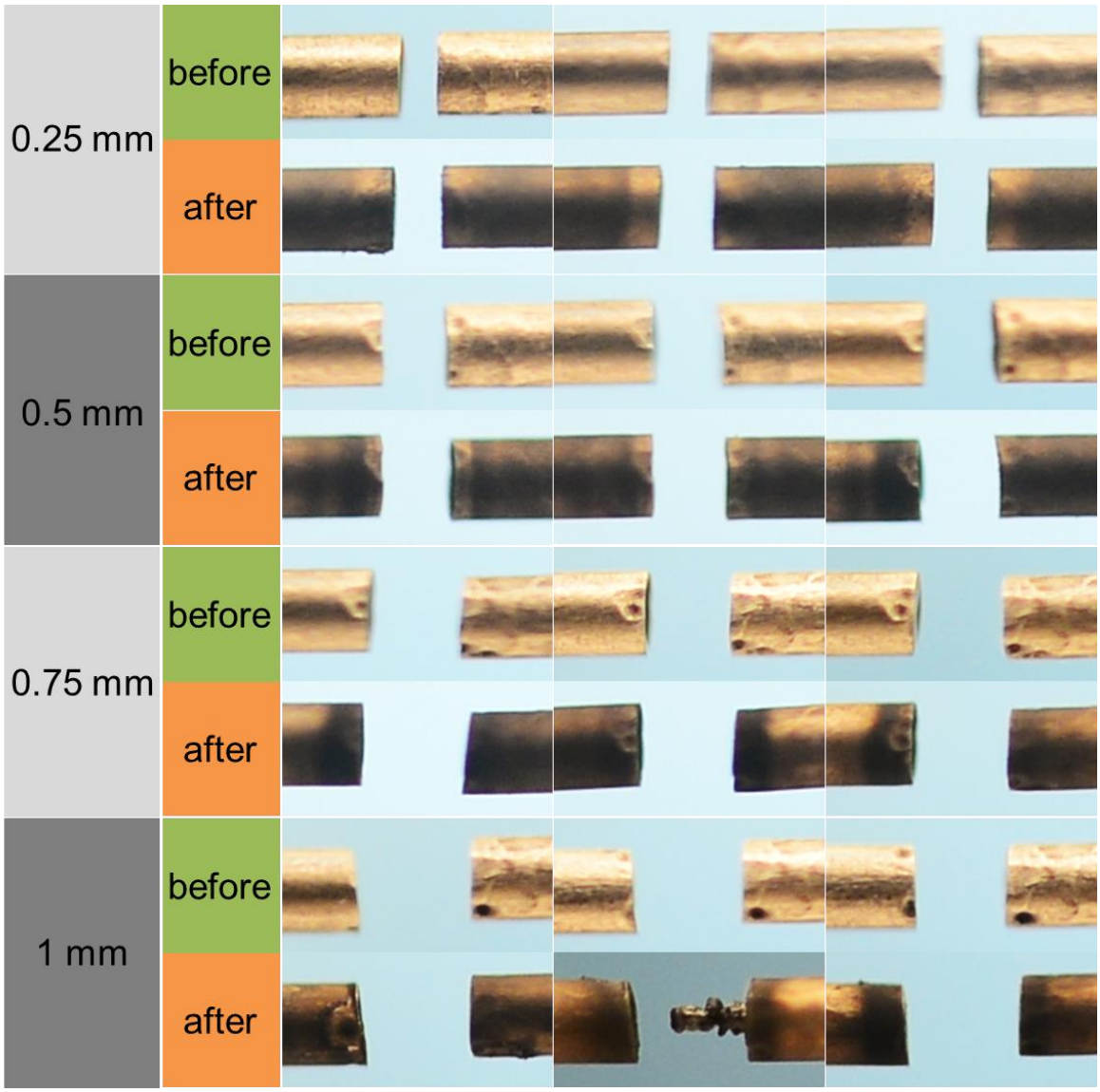

Figure 3-S1 Images of electrode gap distances before and after experiment during 10 minutes discharge by using bipolar pulse power supply at 15 kHz frequency and 1.2 μs pulse width. The diameter of tungsten electrodes were 0.8 mm.

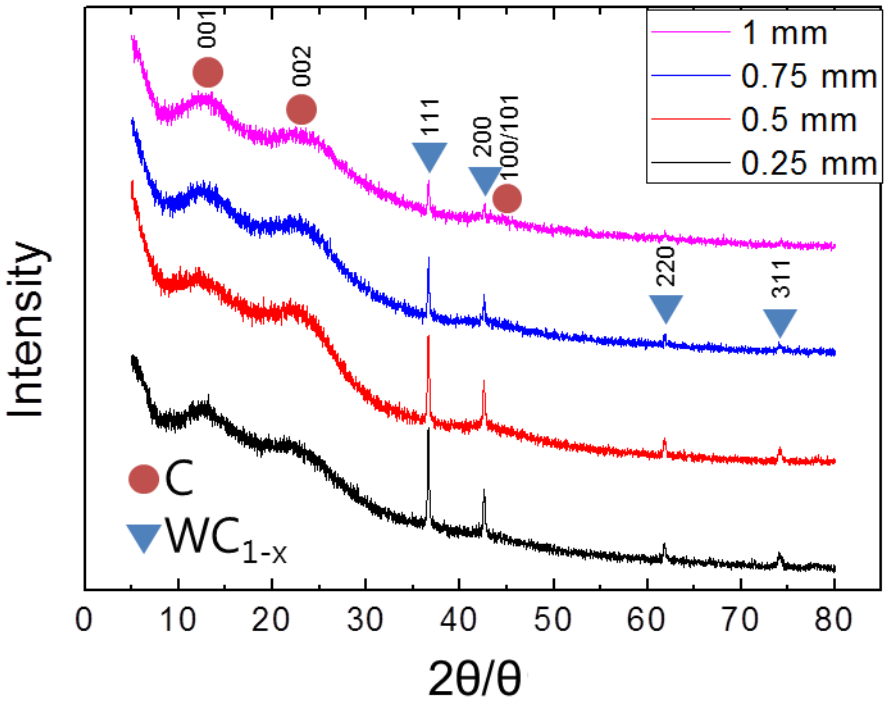

Figure 3-S2 The powder X-ray diffraction (XRD) patterns of as-prepared carbon powders with different electrode gap distances. XRD patterns were recorded in reflection mode (Cu Kα radiation, λ = 1.5418 Å).

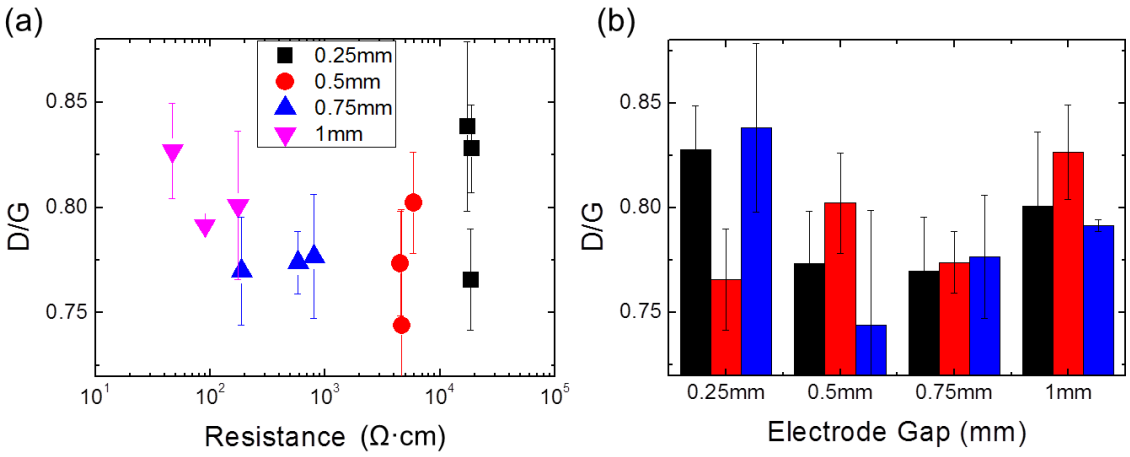

Figure 3-S3 D/G ratio of Raman spectra of as-prepared carbons which were calculated according to (a) resistance and (b) electrode gap. Carbon powders on SiO_2/Si substrate were measured a laser excitation wavelength at 532nm.

Chapter 4

Improvement of Electric Conductivity of Carbon Materials with introducing Naphthalene and Anthracene by Using Solution Plasma Process

Chapter 4 - Improvement of Electric Conductivity of Carbon Materials with introducing Naphthalene and Anthracene by Using Solution Plasma Process

4.1. Introduction

Effective energy distribution and usage are essential issues from the view point of political energy strategy of Japan against global environmental problem. Researches of fuel cell for hydrogen network, secondary battery [3] for energy storage, and super capacitor [4] have been progressed for the energy effectiveness. Among various materials, carbon is mainly used at proton exchange membrane fuel cell (PEMFC) [1,2], condenser and electrode for metal-air battery due to having conductivity and high porosity itself, which helps catalyst particles to disperse in carbon matrix [5-9], effectively.

Carbon materials are synthesized by using various methods such as thermo-decomposition and thermos chemical vapor deposition (thermo-CVD), plasma CVD and so on. Recently, solution plasma method (SP) has attracted big attention at the carbon synthesis [9,14-19].

From now on, through this SP, carbon nanoball (CNB) having high porosity [17], carbon matrix with nano metal catalysts [18] and hetero carbon doped carbon materials [19] have been developed.

SP, which generates low temperature plasma due to long resting time between pulses is distinguished from conventional high temperature plasma using arc discharge [14,20]. Through this SP, carbon material can be synthesized with using chemical reaction between selective molecules as a carbon precusors while carbon material by conventional arc plasma have been obtained through decomposition of carbon precusor and rearrangement between atoms or lower level molecules than

precusor. For example, carbon material can be synthesized by using aromatic compound such as benzene. One of C-H bond of benzene ring can be activated by radical propagation from plasma, and then, the activated benzene radical makes a couple with another benzene molecule. A number of same reactions and chain reaction occurs continuously, carbon materials are obtained with aggregation of small particles in the end. Therefore, properties of carbon material are strongly affected by precursor's original structure. However, this carbon obtained by SP has a problem for immediate use that electric conductivity is quite low because of low effectiveness of dehydrogenation from aromatic ring. Vulcan-XC72 or Ketjen black, which is generally used for electrode material, have resistance value of 0.04 Ωcm and 0.06 Ωcm, respectively, while resistance value of carbon by SP is approximately 100 Ωcm.

In this paper, synthesized carbon by SP through introducing naphthalene and anthracene in benzene solvent was evaluated for improving electric conductivity, because which solutes have more π conjugated sites than benzene.

4.2. Experimental procedure

4.2.1 Material

A total volume of 200 ml benzene (>99.5%, Kanto chemical) was introduced as carbon precu sers. 0.08 mol%,0.39 mol%, 0.76 mol% and 2.54 mol% of naphthalene (>98%, Wako chemic al), and 0.08 mol%, 0.23 mol%, 0.39 mol% and 0.62 mol% of anthracene (>95%, Kanto che mical) was dissolved in benzene, respectively. At this time, 0.62 mol% of anthracene was ma ximum solubility.

4.2.2 Solution plasma process

A schematic diagram of the experimental setup is shown in Fig. 4-1. 0.8 diameter of tungsten electrodes (99.999%, Nilaco Co. Ltd.) were inserted in a total volume of 250 ml teflon reactor. Electrode gap was set at 1 mm during 10 minute discharge, which was generated by using a bipolar pulse power supply (MPP-HV02, KURITA) operated at a voltage between 1 kV and 2 kV, with a frequency of around 15 kHz and a pulse width of around 1.2 μs. After discharge, erosion of electrode gap distance was measured under ±0.05 mm.

Synthesized carbon materials was separated from the solution by filtering through the polytetrafluoethylene (PTFE; JVWP04700, Merck Millipore) membrane filter of 100 nm diameter before drying in the oven at 80 ^{O}C for 24 hours.

4.2.3 Electric conductivity

Electric conductivity of as-prepared carbon powder was measured by using 2 probe measurement. Each sample was placed in a hollow Teflon cylinder (inner diameter = 5 mm), and compressed in air between two commercial brass pistons forming electrode. The load of pressure on the pistons was ~600 kPa by using a hand oil-pressure pump. Fundamental characteristics (discharge voltage and current) were measured by a digital oscilloscope (TDS 3014B; Tektronix).

4.2.4 Structure analysis and chemical composition

Morphology and chemical composition of the synthesized carbon materials were observed and measured by using transmission electron microscopy (TEM, JEOL; JEM-2500SE), X-ray diffraction (XRD, Rigaku; SmartLab X-ray diffractometer) and CHN mass analyzer (Yanaco; MT-6).

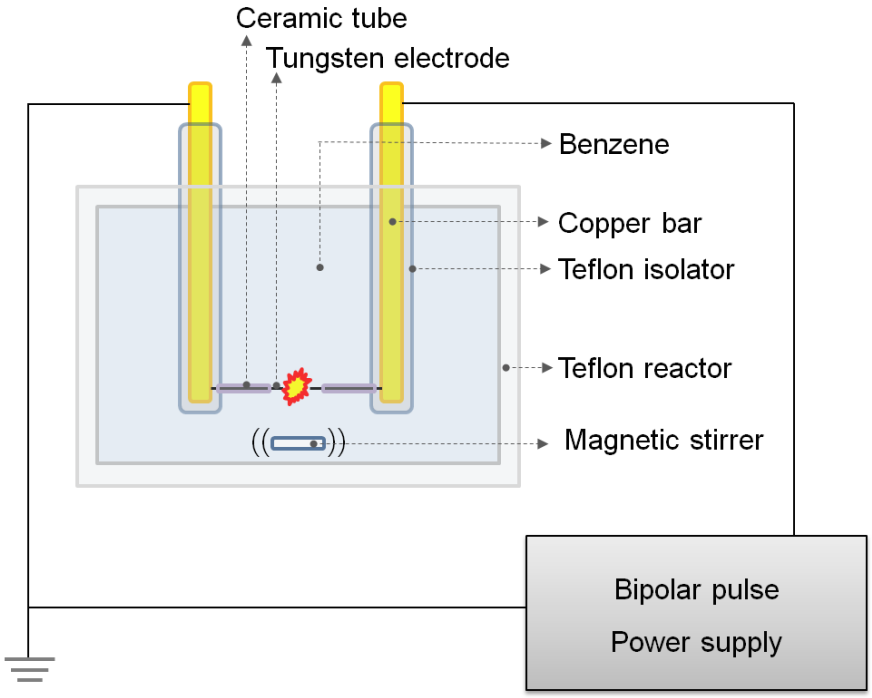

Fig. 4-1 Experimental setup for the solution plasma processing.

4.3. Results

Result of electric resistance of synthesized carbons, after 10 minute discharge in benzene solution introduced solute like naphthalene or anthracene, was shown in Fig. 4-2. Resistance values of obtained carbon from pure benzene solution was 104 (± 65.2) Ωcm. Meanwhile, resistance value of obtained carbon from naphthalene of 0.08 mol%, 0.39 mol%, 0.78 mol% and 1.54 mol% were 85.0 (± 34.4) Ωcm, 47.8 (± 21.3) Ωcm, 37.5 (± 12.1) Ωcm and 26.4 (± 3.0) Ωcm, respectively. In case of obtained carbon from mixed solution with anthracene of 0.08 mol%, 0.23 mol%, 0.39 mol% and 0.62 mol%, the resistance value were measured 75.0 (± 23.1) Ωcm, 32.7 (± 4.0) Ωcm, 20.0 (± 5.0) Ωcm and 16.6 (± 2.8) Ωcm, respectively. These results implied that a little amount of solute effected on resistance of obtained carbon resistance. In addition, anthracene showed more drastic decrease in resistance than naphthalene. By the way, additional experiment in benzene saturated with naphthalene of 19 mol% showed that resistance value of obtained carbon was about 24.5 Ωcm, which confirmed that high concentration of naphthalene had not a strong effect on resistance improvement that much.

H/C ratio of obtained carbon from pure benzene and mixed solution with naphthalene and anthracene was shown in Fig. 4-3. As naphthalene increased in benzene solution, the ratio of H/C in obtained carbon decreased. For example, H/C ratio of obtained carbon from pure benzene was about 0.20 (± 0.02) while that of naphthalene 1.54 mol% decreased about 0.16 (± 0.01). Same tendency appeared in case of anthracene that H/C ratio of anthracene 0.62 mol% was 0.16 (± 0.01). Fig. 4-3(b) showed electric resistance according to H/C ratio of obtained carbon, which suggested that resistance showed small value as H/C ratio became low.

The quantity of obtained carbon with quantity of introduced solute of naphthalene and anthracene in benzene solution was shown in Fig. 4-4. Production rate of obtained carbon increased with concentration of introduced solute. Especially, small amount of anthracene introducing made faster carbon production rate than naphthalene case.

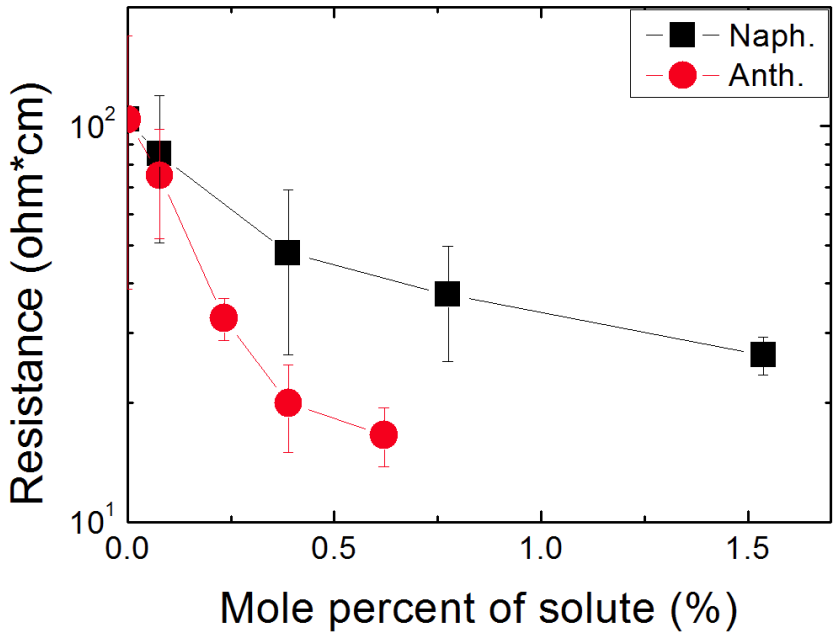

Fig. 4-2 Resistances of carbon powders obtained by using solution plasma process with increase of solute (naphthalene and anthracene) in benzene solvent.

Morphologies of obtained carbon from pure benzene (Fig. 4-5(a)), mixed benzene with naphthalene 1.54 mol% (Fig. 4-5 (b)) or anthracene 0.62 mol% (Fig. 4-5(c)) were shown in Fig. 4-5. The shape of carbon nanosphere (CNS) with size of 20~30 nm, and nanoshape like short range of graphite-like structure were observed in each obtained carbon. By the way, other nanoshape like amorphous structure was often observed in Fig. 4-5(a) as well, which structure was hardly seen in Fig. 4-5(b) and (c).

X-ray diffraction patterns of obtained carbons were shown in Fig. 4-6. All obtained carbon were showed broad peak at 23.4 and 43 of 002 and 100/101 plain, respectively, which

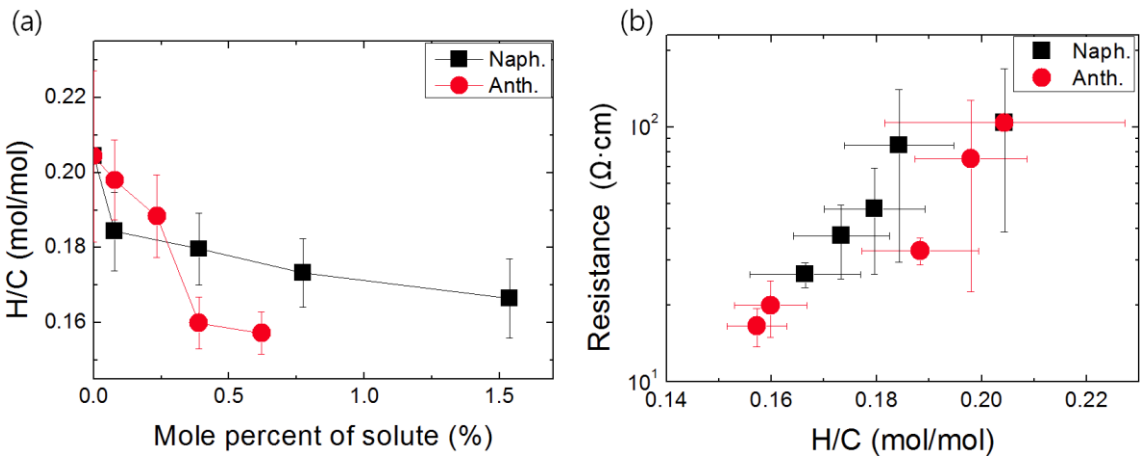

Fig. 4-3 **(a)** H/C ratio of as-prepared carbon powders obtained by using solution plasma process with increase of solute (naphthalene and anthracene) in benzene solvent. (b) H/C ratio also was shown related with resistance value of each one (naphthalene and anthracene).

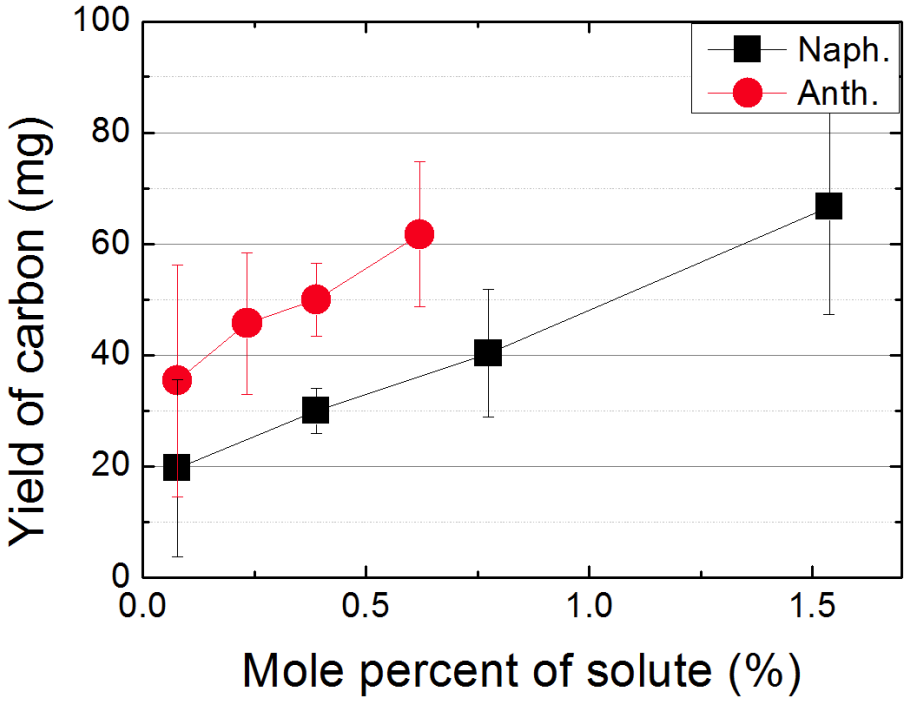

Fig. 4-4 Total yield of obtained carbon powder after 10 minutes discharge according to dissolved quantity of each solute (naphthalene and anthracene).

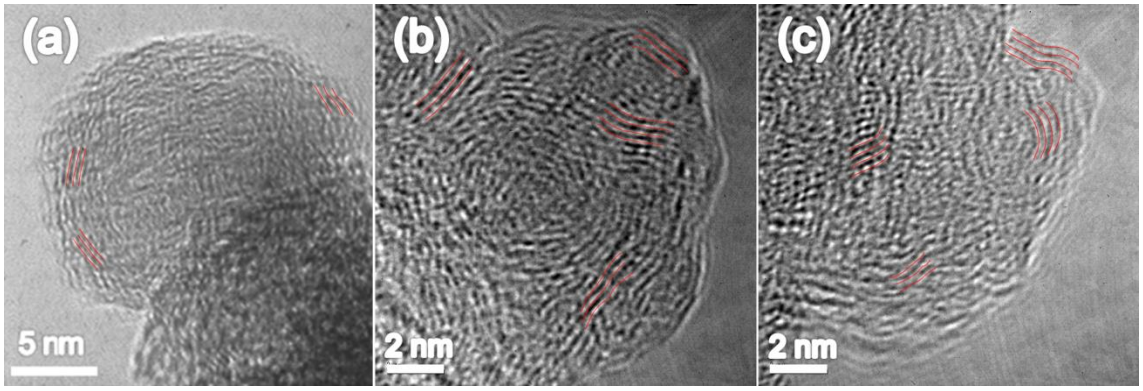

Fig. 4-5 Transmission electron microscopy (TEM) images of as-prepared carbon powers by (a) pure benzene, (b) naphthalene 1.54 mol% and (c) anthracene 0.62 mol%, respectively.

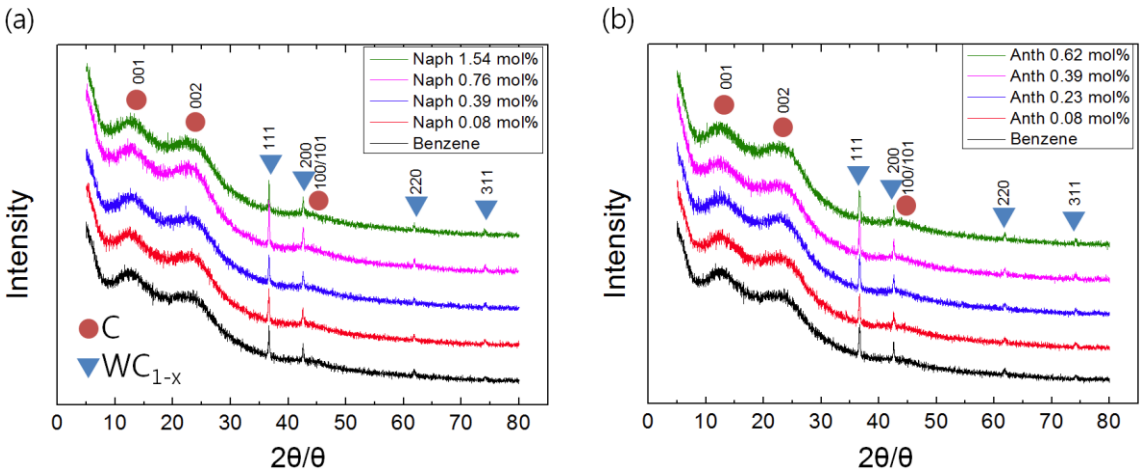

Fig. 4-6 XRD patterns of as-prepared carbon powders with change of each solute ratio ((a) naphthalene and (b) anthracene) in benzene solvent. XRD patterns were recorded in reflection mode (Cu Kα radiation, λ = 1.5418 Å)

suggested that these samples formed turbostratic structures in which small basal planes have slipped out of alignment. However, it was difficult to distinguish detail comparison of crystallinity among samples because the peaks were too broad shapes. This result, as we observed in TEM Fig. 5, could be supposed that crystalline of graphitic structures were too small extent and size in nano level. Other tungsten carbide peaks with sharp shapes were detected at 36.7, 42.4, 61.8 and 74.2 linked with the plains of 111, 200, 220 and 311, respectively. These tungsten carbides came from erosion or sputtering of tungsten electrode by plasma generated in solution. Peak shift or intensity alteration of tungsten carbides according to solute concentration did not appear.

4.4. Discussion

Introducing solute like naphthalene or anthracene in benzene solution brought about lowering H/C ratio, and improving crystallinity and conductivity of carbon material. Especially, small amount of anthracene solute had a noticeable effect on carbon formation. Basically, naphthalene and anthracene have lower H/C ratio than benzene, so that it is not strange that H/C ratio of obtained carbon from introducing naphthalene or anthracene in benzene goes down. However, 0.62 mol% of anthracene was very tiny concentration compared to benzene quantity, and then, measured H/C ratio of carbon was 0.16 (± 0.01) from 0.20 (± 0.02), which made electric resistance change 16.6 (± 2.8) Ωcm from 104 (± 65.2) Ωcm. Resonance energy of naphthalene and anthracene is higher than that of benzene, so that radicals from naphthalene and anthracene could be more stable than benzene radicals. This stability means energy of dehydrogenation reaction goes down. Through higher resonance energy, naphthalene or anthracene originated carbon is supposed to be formed with faster reaction of dehydrogenation, and covalent bond between carbon than that of benzene. Low H/C ratio implied that with large size of carbon domain grew up with fast reaction, which might lead to improve crystallinity and conductivity of carbon materials. This nucleosynthesis reaction was easy to occur with 2 dimensional graphitic shapes during electric discharge because solutes such as naphthalene and anthracene have 2

dimensional molecular structures. These 2 dimensional crystalline nucleuses made it easy to aggregate among themselves after discharge or outside plasma due to high attracting force between interlayers [21]. Obtained carbon quantity increased as well according to high concentration of solute, which indicated that solute had a big roll for formation of carbon materials.

4.5. Summary

Through solution plasma process, enhanced carbon materials with high crystallinity and electric conductivity were synthesized by introducing solutes in benzene solvent such as naphthalene and anthracene, which have π conjugated molecular structures. Little amount of solute gave a significant effect on lowering H/C ratio of obtained carbon, which developed crystallinity of 2 dimensional graphitic structure. In addition, carbon quantity increased as well with high concentration of solutes. Electric resistance of obtained carbon by introducing anthracene was measured around 16.6 Ωcm, which value was 7 times lower than that of about 104 Ωcm from pure benzene solvent.

References

1) J Larminie, A Dicks : Fuel Cell Systems Explained 2nd edition (2003).

2) Y Shao, G Yin, Y Gao ; *J. Pow. Sour.*, 171 (2007).

3) MS Halper, JC Ellenbogen ; Supercapacitors: A Brief Review (2006).

4) A Burke, Z Liu, H Zhao ; Review of the Present and Future Applications of Supercapacitors in Electric and Hybrid Vehicles (2014).

5) C Wang, M Waje, X Wang, JM Tang, RC Haddon, Y Yan ; Nano Lett., 4, 345-348 (2004).

6) C Liu, Z Yu, D Neff, A Zhamu, BZ Jang ; *Nano Lett.* 10, 4863-4868 (2010).

7) Y Wang, Z Shi, Y Huang, Y Ma, C Wang, M Chen, Y Chen ; *J. Phys. Chem.*, 113, 13103-13107 (2009).

8) DN Futaba, K Hata, T Yamada, T Hiraoka, Y Hayamizu, Y Kakudate, O Tanaike, H Hotori, M Yumura, S Ijima ; *Nature materials*, 5, 987-994 (2006).

9) J Kang, OL Li, N Saito ; *J. Power Sources*, 3, 261:156 (2014)

10) A Watanaphanit, N Saito ; *Polym. Degrad. Stab.*, 98, 1072-1080 (2013).

11) P Pootawang, N Saito, O Takai, SY Lee ; *Nanotechnology*, 23, 395602 (2012).

12) SP Cho, MA Bratescu, N Saito, O Takai ; *Nanotechnology*, 22, 455701 (2011).

13) MA Bratescu, SP Cho, O Takai, N Saito ; *J. Phys. Chem. C*, 115, 24569 (2011).

14) OL Li, J Kang, K Urashima, N Saito ; *J. Inst. Electrostat. Jpn.*, 37, 22-27 (2013).

15) HS Lee, MA Bratescu, T Ueno, N Saito ; *RSC advances*, DOI 10.1039/c4ra03253e (2014).

16) G Panomsuwan, N Saito, T Ishizaki ; *Phys. Chem. Chem. Phys.* DOI:10.1039/c4cp05995f (2015).

17) J Kang, OL Li, N Saito ; Carbon, 60, 292-298 (2013).

18) J Kang, OL Li, N Saito ; *Nanoscale*, 60, 292-298 (2013).

19) DW Kim, OL Li, N Saito ; *Phys. Chem. Chem. Phys.*, DOI: 10.1039/c4cp03868a (2014).

20) MA Bratescu, N Saito, O Takai ; Curr. Appl. Phys., DOI: 10.1016/j.cap.2011.06.007 (2011).

21) EG Jones, AK Bhattacharya, TO Tiernan ; *Int. J. Mass Spectrom. Ion Phys.*, 17, 147-161 (1975).

Chapter 5

Summary

Chapter 5 – Summary

Chapter 1 is presents an overview of nano carbon materials to make much more understanding in the overall research. Next, the fundamental and applications of solution plasma process was given in detail.

Chapter 2 describes the synthesis of graphene flakes by SPP process, by controlling the energy input from a bipolar pulsed power supply during solution plasma process in water. The energy per pulse delivered in plasma was similar for both carbon onions and graphene flakes synthesis. However, the power delivered in plasma was much higher in the case of carbon onion synthesis. The main proce ss to produce the carbon onions is carbon vaporization due to Joule effect and carbon recomb ination assisted by plasma. In order to produce graphene flakes, the graphite electrode was exf oliated in plasma. The diameter of the carbon onions was ranged from 2 to 16 nm and the grap hene flakes were hundreds of nanometers in size. Unfortunately a precise control of the latera l sizes and the thickness of the graphene flakes was not realized. The HRTEM, TEM, and EE LS analysis confirmed the morphology and the structure of the graphene flakes and carbon onions. The Raman spectra of the graphene flakes indicated that it was disordered multilayers.

Chapter 3 focuses on the structure-controlled carbon were synthesized by various parameters of SPP. Graphitic carbon structure was synthesized from benzene solvent by using solution plasma process and controlled, especially through adjusting electrode gap distances. This effect plays the important role as the main factor for discharge process in organic solution. TEM and diffraction images of EG 1 showed ordered graphitic layers and clear ring pattern compared with EG 0.25. The only adjustment of electrode gap distance from 0.25 mm to 1 mm had brought about approximately 400 times improvement of conductive property from 19k Ω·cm to 47 Ω·cm. From the result of CHN elemental

analysis, H/C ratio decreased with decrease of resistance from 0.31 to 0.18. The increase of sp2 carbon domains in size may cause to improvement of conductivity.

Chapter 4 presents the effect of introducing solute having more π conjugated sites than benzene and nanocarbon formation mechanism. Through solution plasma process, enhanced carbon materials with high crystallinity and electric conductivity were synthesized by introducing solutes in benzene solvent such as naphthalene and anthracene, which have π conjugated molecular structures. Little amount of solute gave a significant effect on lowering H/C ratio of obtained carbon, which developed crystallinity of 2 dimensional graphitic structure. In addition, carbon quantity increased as well with high concentration of solutes. Electric resistance of obtained carbon by introducing anthracene was measured around 16.6 Ωcm, which value was 7 times lower than that of about 104 Ωcm from pure benzene solvent.

Finally, in this chapter summarized and clarified phenomenon in the plasma discharge in reaction filed, and the way of controlling carbon crystallinity and structures. In this study, we have successfully synthesized conductive carbon having graphitic layers by SPP. The results observed that (1) SPP is a promising method for mass production of carbon and versatile for controlling properties of carbon, (2) conductivity of carbon drastically increased by introducing small amount of precursor having π conjugated sites in benzene and (3) capacity and durability of Li-air battery could be improved without change of properties by heat treatment like aggregation of metal particles and evaporation of nitrogen.

Appendix

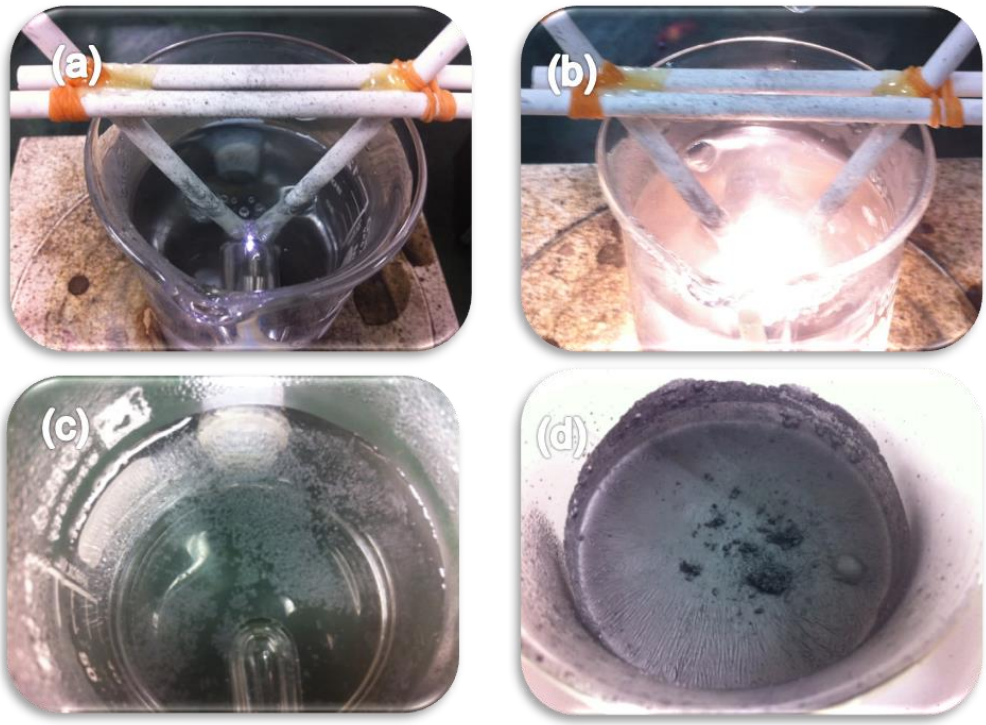

A2-1 Photos of SPP during discharge between graphite electrodes in water with (a) low input energy and (b) high input energy, and obtained carbon materials after discharge with (c) low input energy and (d) high input energy.

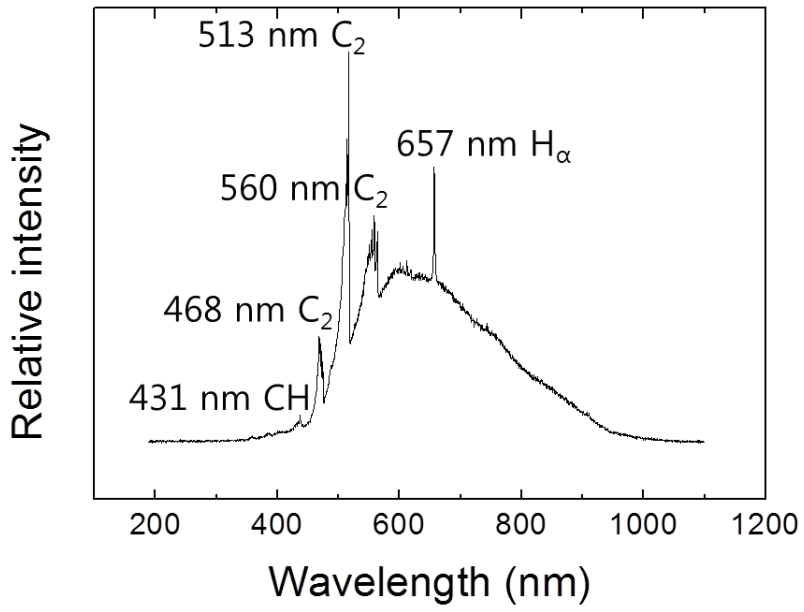

A3-1 Optical emission spectra of plasma generated during the synthesis of carbon in benzene solvent.

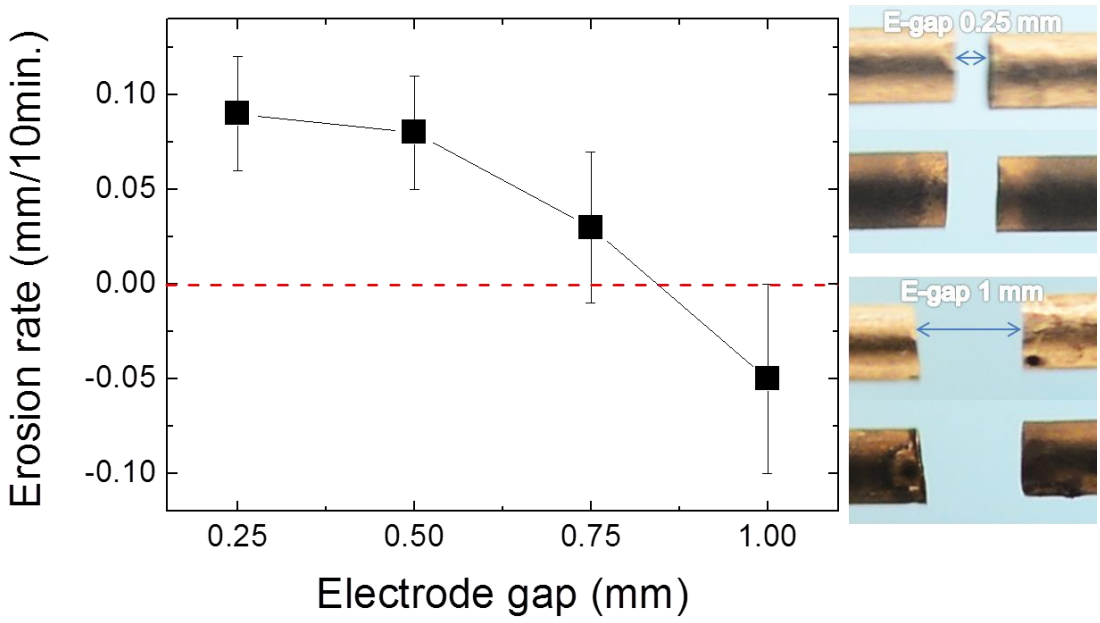

A3-2 Erosion rate of tungsten electrodes at different electrode gap distance after 10 minute discharge in benzene solvent. Minus value means that carbon was deposited on surface of electrode. On the eright side comers, images of electrode gap before and after discharge at EG 0.25 and EG 1.

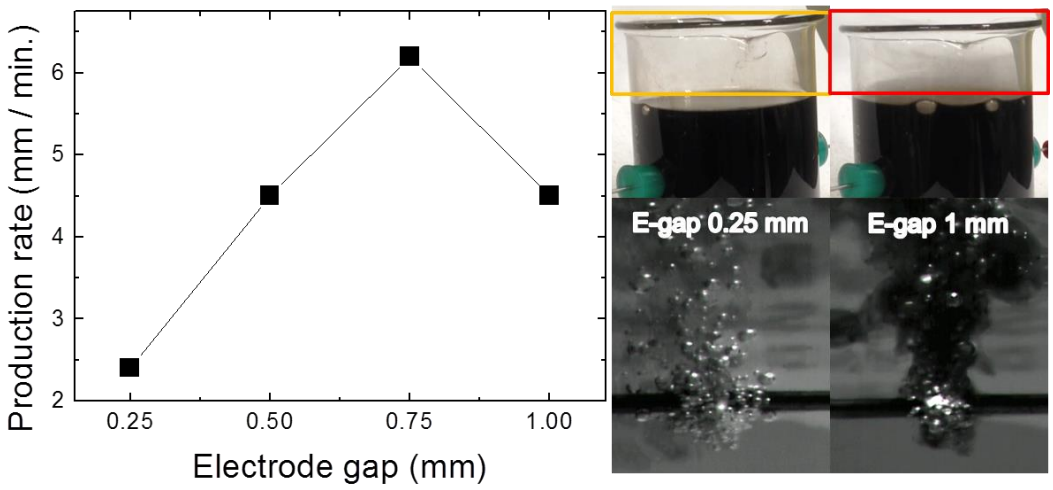

A3-3 Production rate of obtained carbon powder during 10 minute discharge in benzene solvent according to various electrode gap distances. On the right side comers, images of carbon generation in benzene solvent and out of solvent.

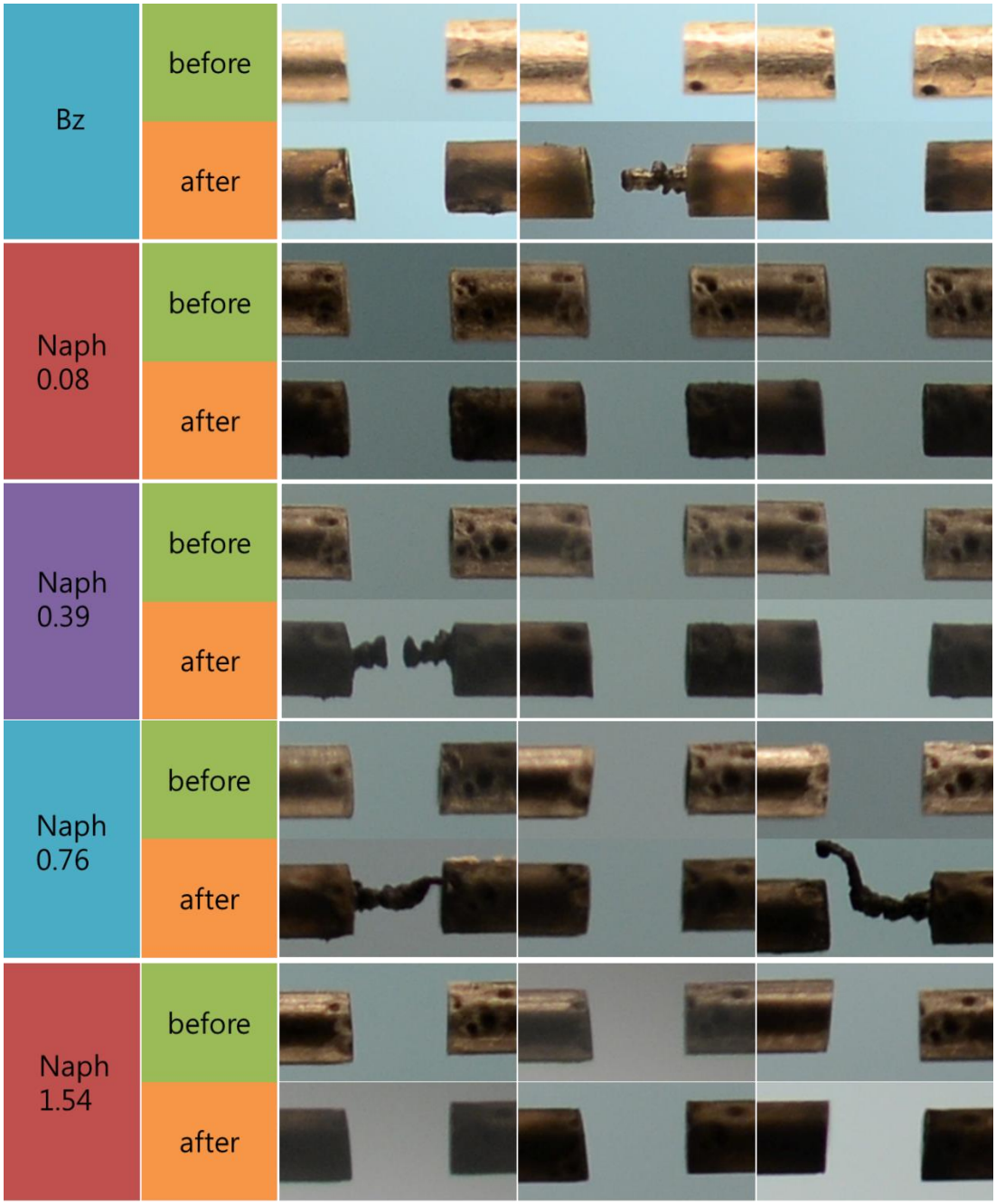

A4-1 Images of electrode in naphthalene introduced benzene before and after experiment during 10 minutes discharge by using bipolar pulse power supply at 15 kHz frequency and 1.2 μs pulse width. The diameter of tungsten electrodes were 0.8 mm, and electrode gap distance was 1 mm.

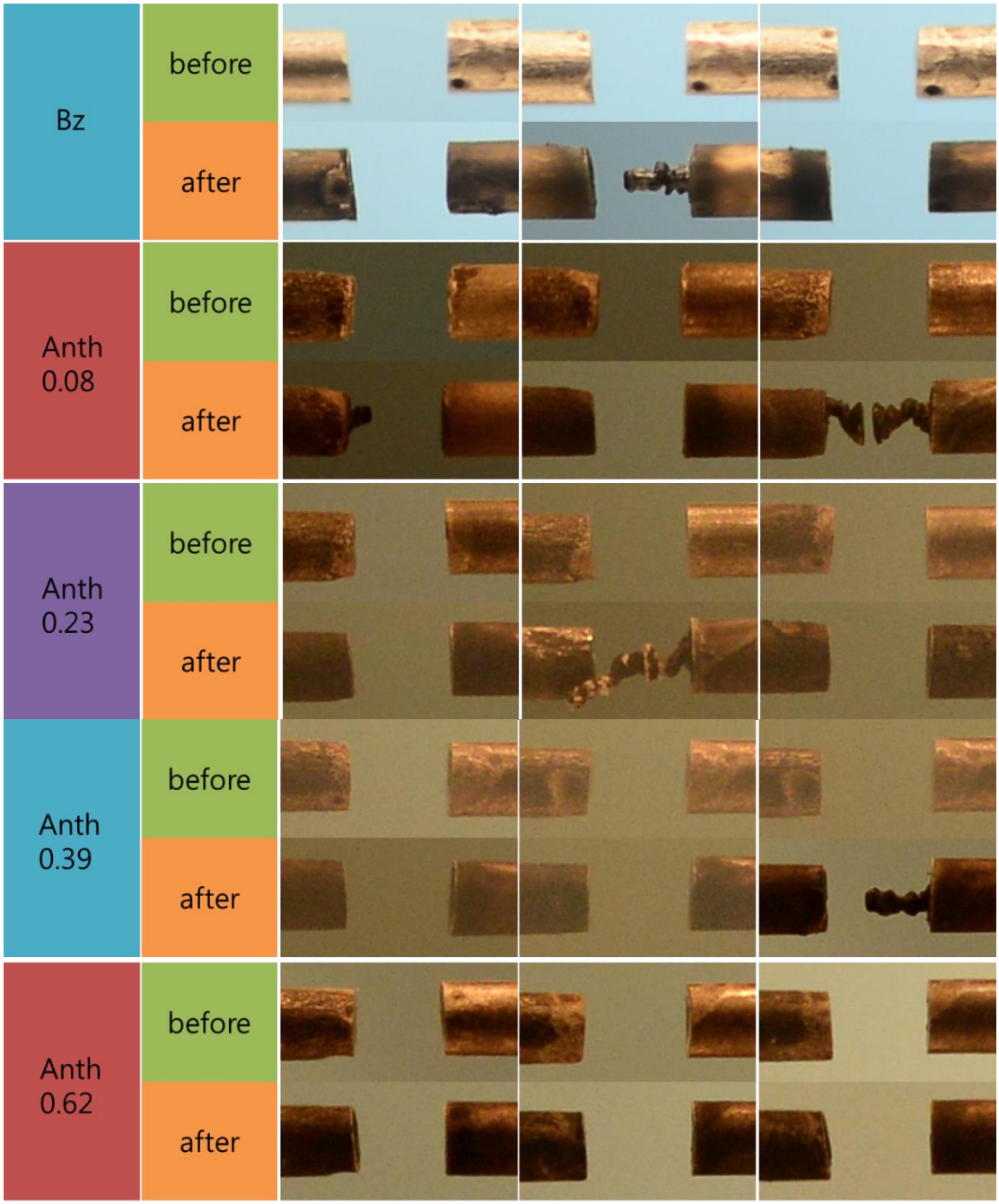

A4-2 Images of electrode in anthracene introduced benzene before and after experiment during 10 minutes discharge by using bipolar pulse power supply at 15 kHz frequency and 1.2 μs pulse width. The diameter of tungsten electrodes were 0.8 mm, and electrode gap distance was 1 mm.

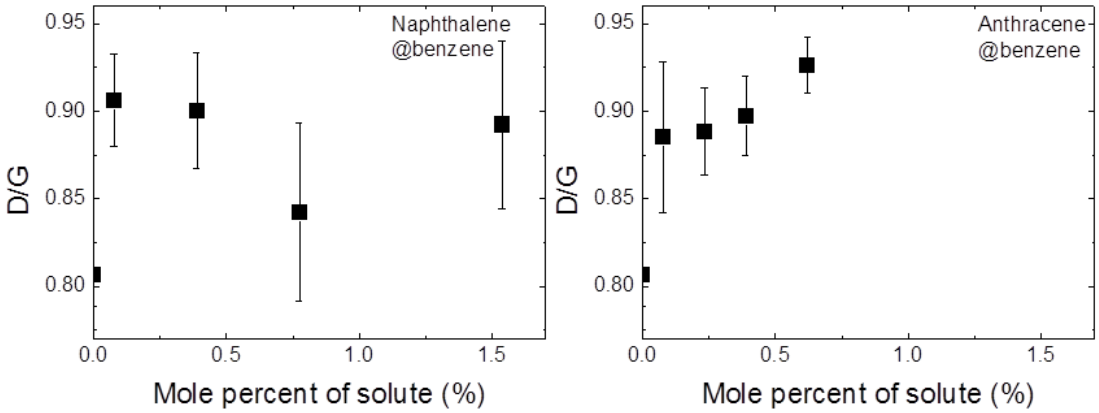

A4-3 D/G ratio of Raman spectra of as-prepared carbons which were calculated according to solute concentrations of (a) naphthalene and (b) anthracene. Carbon powders on SiO_2/Si substrate were measured a laser excitation wavelength at 532nm.

A4-Table 1. Carbon particle analysis by using Brunauer, Emmett and Teller (BET) theory measurement.

20 °C, filter	**Average pore diameter (nm)**	**Pore volume (m^3/g)**	**Surface area (m^2/g)**
Benzene (no filter)	18.847 (20)	1.0379 (0.669)	2.20×10^2 (133.8)
Naphthalene/Bz (1.54 mol%)	12.674	0.8036	2.54×10^2
Anthracene/Bz (0.62 mol%)	13.974	0.9185	2.63×10^2

A. List of publication

Journals

[1] H.S. Lee, T. Ueno, N. Saito, "Solution plasma exfoliation of graphene flaks from graphite electrodes", *RSC Advances*, 4, 51758-65, 2014.

[2] A. Watanaphanit, H.S. Lee, N. Saito, "Cellulose conversion to sugar alcohol by solution plasma processing", *Materials research society proceeding*, Vol. 1745, 1-6, 2014.

[3] H.S. Lee, T. Ueno, N. Saito, "The effect of electrode gap distance on the synthesis of carbon materials by using solution plasma process", *Journal of the minerals, metals and materials society*, Vol. 67, No. 11, 2550-56, 2015.

[4] H.S. Lee, T. Ueno, N. Saito, "Improvement of electric conductivity of carbon materials with introducing naphthalene and anthracene by using solution plasma process", *The Surface Finishing Society of Japan*, 66, 416-9, 2015.

B. List of presentation

International conferences

[1] H.S. Lee, N. Saito, O. Takai, "Catalytic activity of nickel-containing amorphous carbon (Ni:aC) thin films by shielding arc ion plating using bias conditions" *15th International Conference on Thin Films*, 2011.

[2] H.S. Lee, T. Ueno, N. Zettsu, N. Saito, O. Takai, "Chemical structures and mechanical characteristics of a-C and a-CN films by shielding arc ion plating as functions of bias voltages", *International Symposium on EcoTopia Science 11*, 2011.

[3] H.S. Lee, M.A. Bratescu, N. Saito, "Nanocarbon production by solution plasma process in water", *The International Conference on Plasma Nano Technology and Science*, 2013.

[4] H.S. Lee, M.A. Bratescu, N. Saito, "Synthesis of graphene oxide by using solution plasma process in water", *The 13th International Symposium on Biomimetic Material Processing*, 2013.

[5] H.S. Lee, M.A. Bratescu, N. Saito, "Synthesis of graphenes and carbon onions produced by bipolar electrical discharges in water", *MHS2012/Micro-Nano GCOE*, 2012.

[6] H.S. Lee, M.A. Bratescu, N. Saito, "Catalytic activities of metal/carbon compound used by vacuum and solution plasma process", *AVS 59th International Symposium and Exhibition*, 2012.

[7] H.S. Lee, M.A. Bratescu, N.Saito, "Electric and chemical properties of granulated metal/a-C films deposited by shielding arc ion plasma", *International Union of Materials Research Society International Conference in Asia*, 2012.

[8] H.S. Lee, M.A. Bratescu, N. Saito, "Structural control of graphenes and carbon onions by solution plasma process in water", *International Symposium on Micro-Nano systems for the interaction of Young Researchers in Nagoya*, 2012.

[9] H.S. Lee, M.A. Bratescu, N. Saito, "Nanocarbon production by solution plasma process in various solutions", *ISPlasma2013*, 2013.

[10] H.S. Lee, M.A. Bratescu, N. Saito, "Nanocarbon production by solution plasma process in water", *IC-PLANT2013*, 2013.

[11] H.S. Lee, M.a. Bratescu, T.Ueno, N. Saito, "Exfoliation of graphene sheets from graphite electrode in water, "*MHS2013 & Micro-Nano Excellent Graduate School*, 2013.

[12] H.S. Lee, T. Ueno, N. Saito, "Exfoliation of graphene sheets from graphite electrode by solution plasma process in water", *International Conference on Surface Finishing (ICSE2013)*, 2013.

[13] H.S. Lee, M.A. Bratescu, T. Ueno, N. Saito, "Synthesis of graphene sheets from graphite electrode in water using solution plasma exfoliation" *ISPlasma2014/IC-PLANT2014*, 2014.

Domestic conferences

[1] H.S. Lee, N. Saito, O. Takai, "Morphology and adhesion properties of amorphous carbon films by shielding arc ion plating using bias conditions", *The 124th Surface Finishing Society of Japan*, Oral presentation, 2011.

[2] 李　熏聲、上野　智永、是津　信行，齋藤　永宏、高井　治，"アークイオンプレイティング法を用いて成

膜した金属/アモルファスカーボンフィルムの電気化学的特性”, 資源・素材学会春季大会, 2012.

[3] H.S. Lee, T. Ueno, N. Zettsu, N. Saito, O. Takai, “Granulated metal/a-C films deposited by shielding arc ion plating”, *The 125th Surface Finishing Society of Japan*, 2012

[4] H.S. Lee, M.A. Bratescu, N. Saito, “Granulated metal/a-C films deposited arc ion plating”, *The 126th Surface Finishing Society of Japan*, 2012.

[5] H.S. Lee, M.A. Bratescu, N. Saito, “Structural properties of nanocarbon materials by solution plasma process in water”, *The Surface Finishing Society of Japan*, 2013.

[6] リ　フンソン、上野　智永, 齋藤　永宏, “ナフタレンおよびアントラセンの微量添加によるソリューションプラズマ合成カーボン材料の導電性向上”, 第132回表面技術学会春季大会, 2015.

[7] H.S. Lee, T. Ueno, N. Saito, “Control of carbon conductivity with induction of naphthalene and anthracene by using solution plasma”, *The 76th JSAP Autumn Meeting*, 2015.

Acknowledgements

I want to say my thanks to Prof. Nagahiro SAITO (Institute of Innovation for Future Society and Graduate School of Engineering, Nagoya University). He gave me special opportunity. For example, I could study in an unforgettable research environment and I was received his kind advices, support, and encouragement when I was in Nagoya University. I also want to say my deep appreciation to Assistance Prof. Tomonaga UENO (Green Mobility Collaborative Research Center, Nagoya University) for his invaluable comments, and continuous encouragement. I should show my huge appreciation to Prof. Oi Lun Li Helena (Department of Material Science, Nagoya University) and Prof. Anyarat Watthanaphanit (Department of Material Science and Engineering, Nagoya University). They gave me lots of inspiration to extent my knowledge and supported me with their earnest guidance. I would like to say thank you to Prof. Ryoichi ICHINO (Institute of Materials and Systems for Sustainability, Nagoya University), Prof. Noritsugu UMEHARA (Graduate School of Tribological Engineering, Nagoya University), and Prof. Naoto OHTAKE (Graduate School of Science and Engineering, Tokyo Institute of Technology). They reviewed this thesis gladly and gave me valuable comments.

I should not forget to thank to Prof. Myeong-Hoon LEE (Korea Maritime University). He was my great map and compass when I was in master's course, so I received a lot of honest encouragement from him.

I should say my sincere appreciation and thank to all the members of SAITO laboratories of all researchers and graduate students. Especially, I want to say my special thanks to Prof.

Maria Antoaneta BRATESCU for her advice on research. Thanks also to Dr. Shoji NODA for his many kindnesses. I want to say my special thanks to Prof. Jun KANG (Korea Maritime University), Dr. Panuphong POOTAWANG, Dr. Gasidit PANOMSUWAN, Dr. Daewook KIM (Shinshu University), Mr. Wattanachai YAOWARAT, Mr. Akceoglu GARBIS, Mr. Tomohito SUDARE, Mr. Koangyong HYUN, Ms. Seunghyo LEE, Ms. Hyemin KIM, Mr. Kyusung KIM. We have spent much time in Saito Lab., and had unforgettable livings together.

Finally, my great-great special thanks must go to my parents, Gyuhyoung LEE and Hojung KWON, for their constant encouragement and support throughout the past years.

2015

Hoonseung LEE